International Journal of Heat and Mass Transfer 88 (2015) 735–754

Contents lists available at ScienceDirect

International Journal of Heat and Mass Transfer

journal homepage: www.elsevier.com/locate/ijhmt

Review

Summary and evaluation on single-phase heat transfer enhancement techniques of liquid laminar and turbulent pipe flow

Wen-Tao Ji [a,b], Anthony M. Jacobi [b], Ya-Ling He [a], Wen-Quan Tao [a,*]

[a] Key Laboratory of Thermo-Fluid Science and Engineering of MOE, School of Energy and Power Engineering, Xi'an Jiaotong University, Xi'an, China
[b] Department of Mechanical Science and Engineering, University of Illinois at Urbana-Champaign, Urbana, IL, USA

ARTICLE INFO

Article history:
Received 23 December 2014
Received in revised form 29 March 2015
Accepted 2 April 2015
Available online 22 May 2015

Keywords:
Turbulent convection
Heat transfer enhancement
Pipe flow
Performance evaluation

ABSTRACT

A comprehensive literature survey on the thermal–hydraulic performance of liquid flow and heat transfer in pipes with internal integral-fins, twisted tape inserts, corrugations, dimples, and compound enhancement techniques is conducted in this paper. The results of recent published papers with the developments of each technology are also included. It is found that for turbulent heat transfer the enhancement ratio of experimental Nusselt number over Dittus–Boelter equation for internal integral-finned tube is generally in the range of 2–4; twisted tape insert is 1.5–6; corrugated tube is 1.5–4 and dimpled tube is 1.5–4, including the compound enhancement techniques. The ratio of experimental friction factor over Fanning equation is mostly in the range of 1–4 for tubes with internal integral-fins, 2–13 for inserted twisted tape, 2–6 for corrugated tube and 3–5 for dimpled tube. The internally-finned tubes yield the best thermal–hydraulic performance compared with the other three types of tube, whose heat transfer rate augmentation over plain tube is more than the increase of friction factor at the same flow rate. For most of the corrugated and dimpled tubes, the heat transfer enhancement ratios are larger than the increment of pressure drop penalties. For the twisted tape inserts, the pressure drop is remarkably increased at the turbulent flow, and most of data have lower efficiency than the other three types of tube, while it is found to be effective in laminar and transition flow and higher viscosity fluid.

Contents

* Corresponding author.
E-mail address: wqtao@mail.xjtu.edu.cn (W.-Q. Tao).

http://dx.doi.org/10.1016/j.ijheatmasstransfer.2015.04.008
0017-9310/

Nomenclature

a	side length of equilateral triangle in the coiled wire cross section, m
A_n	nominal heat transfer area based on the internal diameter as if the fin structure were not present, m^2
A_a	actual heat transfer area, m^2
A_{fa}	actual flow area, m^2
A_{fc}	core flow area through an internally finned tube, m^2
A_{fn}	nominal flow area based on the internal diameter as if the fin structure were not present, m^2
A_{fin}	inner fin flow area through an internally finned tube, m^2
$\overline{B}(e^+,\alpha)$	friction factor correlating parameter for helical-rib roughness, dimensionless
$\overline{B}(e^+)$	friction factor correlating parameter for geometrically similar roughness and friction similarity function, dimensionless
c	distance between inner wall of the tube and twisted tape insert, m
d_i	inside diameter of the tube, m
d_h	hydraulic diameter, m
d_p	diameter of dimples, m
e^+	roughness Reynolds number $(e/d_i)\mathrm{Re}(f/2)^{1/2}$, dimensionless
e	absolute roughness (fin height), m; Fin height on the twisted tapes, m; wire diameter, m
E	inserted tape-to-tube wall gap thickness, m
F	function in the correlation of Carnavos [37] (1980)
f	Fanning friction factor
Gr	Grashof number, $g\rho^2 d_i^2 \beta \Delta T_w/\mu^2$
$\overline{g}(e^+)$	heat transfer correlating parameter for geometrically similar roughness, dimensionless
Gz	Graetz number
H	non-dimensional fin height $(2e/d_i)$, pitch for 180-deg rotation of tape, dimensionless
l_c	characteristic length, m
l_{mc}	modified characteristic length for swirling flows, m
L	length of test section, m
L_p	protrusion spacing, m
$\dot{m}$	flow rate, m^3/s
n	index of Prandtl number in Dittus–Boelter equation
N_s	number of starts
Nu	Nusselt number
Nu_i	axially averaged Nusselt number based on internal diameter of the tube
p	rib pitch, m
p_a	axial pitch of fins, m
p_c	circumferential pitch of fins, m
Pr	Prandtl number
ΔP	pressure drop, Pa
Ra	Rayleigh number, $Gr \cdot \mathrm{Pr}$
Re_{ax}	Reynolds number based on axial velocity, $\rho V_a d_i/\mu$
Re_i	Reynolds number based on internal diameter of the tube
Re_s	swirl flow Reynolds number
SW	modified non-dimensional axial pitch $(N_s \sin\alpha/\pi)$
s	mean fin thickness, (m)
t_b	fin base thickness, (m)
t_t	fin tip thickness, (m)
u^*	shear velocity, m/s
u	fluid velocity, m/s
V_a	mean axial velocity for internal twisted tape tube, $m\cdot/\rho A_c$, $A_c = (\pi d_i^2/4) - \delta d_i$, m/s
X_f	functions in the correlation of Wang et al. [36] (1996)
w	fin width, m; Width of twisted tapes, m, Width of indent, m
W	non-dimensional internal flow area $((\pi/N_s - s/d_i)\cos\alpha)$
Y_b, y_g	functions in the correlation of Wang et al. [36] (1996)

Greek alphabet

α	helix angle, (°)
β	flow attack angle, (°)
v	kinematic viscosity, m^2/s
θ	fin apex angle or rib included angle in [38], (°)
λ	thermal conductivity, W/m·K
δ	tape thickness, mm
δ_t	wall thickness, mm
ρ	fluid density, kg/m^3
μ	fluid dynamic viscosity, $(N\cdot s)/m^2$
τ	apparent wall shear stress, $\tau_o = -\frac{d_i dP}{4dx}$

Subscripts

c	corrugated tube
d	dimpled tube
f	fluid or internally finned tube
r	reference(plain) tube
s	smooth tube
t	tape inserts
w	tube wall

1. Introduction

Heat transfer in pipe flow is widely used in refrigeration, air conditioning, power, chemical and petrochemical industries. Various augmentation techniques have been utilized to enhance the single-phase convection heat transfer of pipe flow. Enhancement of heat transfer can reduce the size of heat exchangers, provide higher heat transfer efficiency, and yield savings of operating costs and materials. A great number of researches has been made on different kinds of pipe flow enhanced techniques. The major results of enhancement study, either numerical or experimental, are often expressed by two ratios, friction increase

ratio and heat transfer enhancement ratio. According to [1,2], heat transfer enhanced ratios can reach as high as 6.0 compared with plain tube.

To the authors' knowledge, the first survey on the techniques to enhance single phase forced convection heat transfer was made by Bergles and Morton in 1965 [3]. In their paper, the enhancement techniques were classified into passive and active methods. The passive enhanced techniques include: (1) Artificial surface roughness, including protrusions, sand grains, and knurling; (2) Displaced promoters, such as flow disturbers located away from the heat transfer surface; (3) Vortex generators, like twisted tape insert, coiled wires inserts, threads, internally coiled tubes. According to the review, the heat transfer enhanced ratio of rough surface was around 2-fold compared with smooth surface. For the displaced promoters, the highest heat transfer enhanced ratio in the survey was 1.4. Turbulence promoters had generally higher enhanced ratio than those encountered with surface roughness elements and displaced turbulence promoters. The best enhancement ratio in the survey was 2.1–2.8. Since the pioneering work of [3], numerous review papers for the enhancement of single phase heat transfer technologies have been published, to name a few, Refs [4–14] can be consulted.

It is a well-known fact that any enhancement technique will introduce additional fluid pressure drop, and often the ratio of pressure drop increase is larger than that of heat transfer enhancement. Hence it is very important on how to quantitatively evaluate the thermo-hydraulic performance improvement for a given enhancement technique. Performance evaluation is normally made by comparing the performance of the enhanced surface with a corresponding referenced structure. In all the aforementioned papers comparisons of enhanced technique and referenced structure were usually conducted for heat transfer and friction factor separately. Some thermal–hydraulic performance comparisons were made either using j/f as a criteria [15] or using quite complicated criteria [16], where 12 different cases were proposed for comparison. With the emerging of world wide crisis of energy shortage, energy-saving has become the major purpose of heat transfer enhancement study. Thus it is rational to take the following three constraints as comparison criteria: comparing the enhanced surface with the reference one for (1) identical pumping power; (2) identical pressure drop, and (3) identical flow rate. Recently Fan et al. proposed a performance comparison approach in [17] which combines the three constraints and expresses the comparison results in the same plot. This comparison approach will be adopted in this paper. It should be noted that Li et al. [18] adopted this approach for comparing 27 techniques used in gas compact heat exchangers and very recently He and Tao [19] adopted this approach to compare quite a few enhanced techniques, including internal flow and external flow, gases and liquids. In this paper the focus is put on a systematic comparison of enhanced techniques for liquid heat transfer in tubes.

For internal pipe flow, it might involve three types of heat transfer intensification techniques. They are two-dimensional roughness, three-dimensional roughness, and compound techniques. Internal integral-fin, twisted tape inserts, corrugations, and twisted structure typically belong to two dimensional roughness. The dimpled tube belongs to three dimensional roughness. Two or more techniques are often utilized simultaneously and such combination is called compound techniques. Three dimensional roughness, internally grooved fin, twisted tape insert, wavy and dimple are the most widely used techniques to enhance the liquid pipe flow heat transfer.

There are numerous investigations, both experimental and numerical, on the enhancement of turbulent pipe flow heat transfers. In this paper, only the experimental results of the most commonly used techniques are reviewed and compared. These include internal integrally finned, twisted tape and coil inserted, corrugated, twisted, dimpled, and three dimensional roughed tubes. In order to determine which types of enhanced form or structure has a higher efficiency, the thermo-hydraulic performance of the enhanced technique is evaluated with performance evaluation plot proposed by Fan et al. [17]. In their plot $\lg(Nu_e/Nu_r)$, $\lg(f_e/f_r)$ are taken as the ordinate and abscissa, respectively. Every enhancing technique can be expressed in the figure and under what constraint the technique will enhance heat transfer can be clearly identified. For the simplicity of presentation the assumptions and details of plot construction of [17] are omitted here. It can be confirmed that all the techniques and related test data compared in this paper satisfy the assumptions made in [17] .

The following presentation is divided into five sections: internally integral finned tube is reviewed and evaluated in Section 2; Section 3 is for internally inserted tapes and coils. In Section 4, corrugated and twisted tubes are presented; dimpled and the tube surface with three dimensional protrusions are summarized in Section 5; and finally, some conclusions are made in Section 6.

2. Internal integral fins

2.1. Introduction of internal integrally-finned tubes

Internal fin is one type of turbulence promoter to enhance the forced convection heat transfer. As shown in Fig. 1, a certain number of protruding rigs is machined based on tube wall. Either transverse or helical repeated ribs can be manufactured. Featured by relatively low cost of production, reliability and low pressure drop, it has been ever-increasingly adopted in many engineering applications. The weaknesses of the internal integral finned tubes are the fouling and lower heat transfer enhanced ratio at laminar and transition flow region [20]. It is usually used in the systems where liquids must be as clean as possible such as air-conditioning systems and refrigeration industries.

As indicated in [21–25], the basic methods for intensification of single phase heat transfer is increasing turbulence and convective mixing. The fluid flow close to tube wall plays an important role in the enhancement of heat transfer. When fluid flows directly across the helical fin, favorable pressure gradient accelerates fluid flow before fin tip. After the fin tip, it is against an adverse pressure

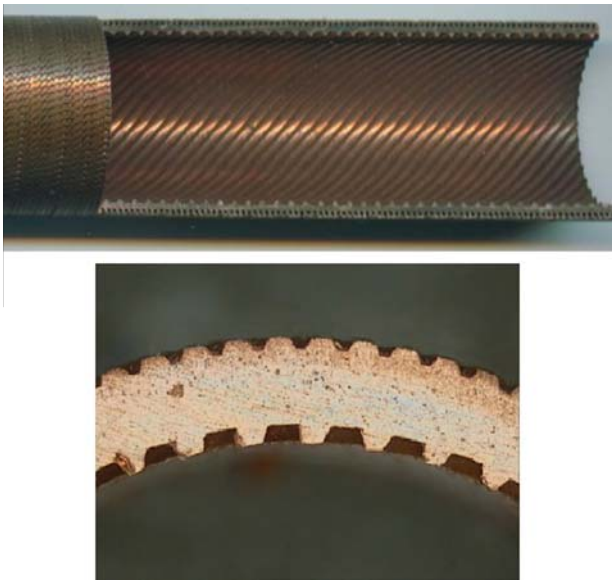

Fig. 1. Internal helically finned tubes.

gradient and the speed of boundary layer relative to the fin decreases. The velocity boundary layer may detach from fin surface, leading to a separated flow. Swirling vortex may generate after the rib close to tube wall. The disturbed condition promotes the convection heat transfer but also results in a penalty in pressure drop. Additional pressure drop is induced between the front and rear of fins.

As depicted in Figs. 1 and 2, the geometric parameters of finned tube include the internal diameter of tube (d_i), inner fin height (e), number of starts (N_s), helix angle (α), fin base thickness (t_b), and fin pitch (p, $\pi d_i/N_s$). Typically, the parameters of internally-fined tube are in the range of $0.01 \leqslant e/d_i \leqslant 0.4$, $1 \leqslant N_s \leqslant 82$, $1.5 \leqslant p/e \leqslant 46.7$, $1.5 \leqslant t_b/e \leqslant 2.5$, and $0° \leqslant \alpha \leqslant 90°$ [20,26–28]. High fins are primarily used for fluids that have lower convective heat transfer coefficients or that with high viscosity. For the fluid flow with higher Reynolds number such as water, micro-finned tubes are widely used in engineering applications. The above parameters have significant effects on heat transfer coefficient in the turbulent flow regime. With the increment of e/d_i, N_s, or α, both the friction factor and Nusselt number increase [29–31], and the effects are nonlinear.

2.2. Correlations for average heat transfer coefficient and friction factor

There are plenty of experimental and theoretical investigations on the heat transfer of internally finned tube in turbulent flow. However, because of the complexity of turbulent flow, the predictions on the heat transfer and friction factors still mostly rely on empirical correlations. The correlations can be derived from similarity theory or dimensional analysis based on the experimental data. A comprehensive review on the correlations of internally grooved tubes is presented in Table 1. The related predicting accuracy, scope of geometric and flow parameters are also provided.

The correlation for friction factors of internally roughed tube was firstly established by Nikuradse [32] in 1933. The general expressions of velocity distribution and law of resistance were given in the paper. The friction similarity law of Nikuradse is written as:

$$\overline{B}(e^+) = \sqrt{2/f} + 2.5\ln(2e/d_i) + 3.75 \tag{1}$$

where e^+ is the roughness Reynolds number, $e^+ = \frac{eu^*}{v} = \frac{e\tau_w/\rho}{v} = (e/d_i)Re\sqrt{f/2}$, and $\overline{B}(e^+)$ is a friction similarity function determined empirically. It is a constant of 8.48 when $e^+ > 70$.

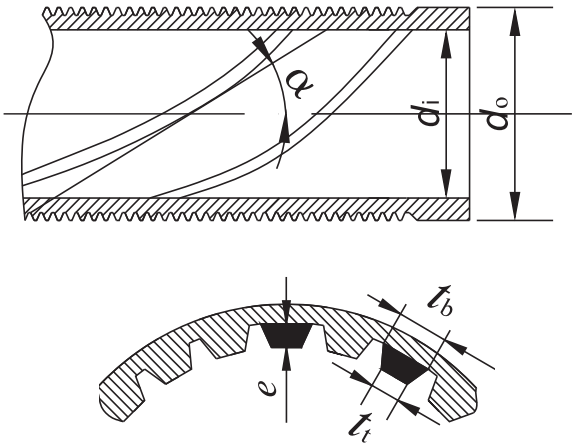

Fig. 2. Schematic diagram of internally finned tube.

A more general heat transfer similarity relation for smooth and rough tubes was developed by Dippery and Sabersky [33]. It was complimentary to Nikuradse's friction similarity law. It is written as:

$$Nu = \frac{(f/2)\mathrm{RePr}}{1 + \sqrt{f/2}[\overline{g}(e^+)\mathrm{Pr}^n - \overline{B}(e^+)]} \tag{2}$$

where $\overline{g}(e^+)$ is a dimensionless heat transfer similarity function. A set of experiments was required for each types of roughness to determine $\overline{g}(e^+)$. Webb [26] suggested that the heat-momentum transfer analogy should be applicable to any basic type of roughness. This equation was used to correlate data of both the transversely and helically finned tubes. The correlations of Webb et al. [26], Han [34], Gee and Webb [35], Wang et al. [36], listed in Table 1 were all primarily originated from Eqs. (1) and (2).

The correlations were also obtained by regression of experimental data among some dimensionless parameters. Heat transfer characteristics of water, air and 50% ethylene glycol(EG)-water solution in turbulent flow were experimentally tested by Carnavos [37] for 11 tubes having longitudinal and helical integral fins. The parameter of actual flow area, and core flow area, nominal heat transfer area, and actual heat transfer area are used in the equation. The equation can predict data of air, water, and ethylene glycol–water solution within ± 10% for the range listed in Table 1, and works well on tubes with a higher helix angle and a larger internal heat transfer surface area. However, for the tubes with higher helix angles and lower Reynolds numbers, the deviations become more pronounced.

Nusselt number and friction factor were also correlated with N_s, e/d_i, p/e, and α, the detailed geometric parameters. The equations of Ravigururajan and Bergles [27], Webb et al. [38] are all belong to this type. The correlations of Ravigururajan and Bergles [27] were based on the experiments of 17 research papers with internally finned geometry of e/d: 0.01 to 0.2; p/d: 0.1 to 7.0; α/90: 0.3 to 1.0; Re: 5000 to 250,000, and Pr: 0.66 to 37.6. It was claimed that the equation for f could predict 96% of the database (1658 points) within the deviations of ± 50% and 77% database within ± 20% deviations. For the equation of Nusselt number, prediction results was within ± 50% for 99% of the data (18070 points) and 69% within ± 20%. For the equation of Webb et al. [38], the deviations were claimed within 2.9 and 3.8 percent for friction factor and Nusselt number, respectively, of 7 tubes.

A comprehensive database of friction factor for internal microfin tubes was established by Wang and Rose [39]. The data were directly read from the figures of literatures for water, R11, and ethylene glycol. They include 21 tubes with inside diameter from the fin root between 6.46 and 24.13 mm, fin height between 0.13 and 0.47 mm, fin pitch between 0.32 and 1.15 mm, and helix angle between 17 and 45 degrees. The database were used to evaluate the friction correlations of Carnavos [37], Ravigururajan and Bergles [27], Wang et al. [36], Jensen and Vlakancic [29], and Webb et al. [38]. They indicted that the correlation of Jensen and Vlakancic[29] was the best and represented most of the database within ± 21% deviation. The others were found to be in good agreement only in a certain range.

Generally, the increase in friction factor leads to an increment on heat transfer for internally grooved tubes. The ratios of heat transfer enhancement were approximately the same as the ratio of friction factor increase for the internally micro-finned tubes in turbulent flow [28,38]. The equation of Ji et al. [40] was simply based on this assumption. The equation for predicting the average heat transfer of inner helically micro-finned tubes was proposed based on Gnielinski equation with the friction factor in the numerator of the original Gnielinski equation being replaced by the measured friction factor in the fully developed turbulent flow region of

Table 1
Correlations for internally grooved tubes.

Authors	Tube geometry/Fluid	Validation range	Friction	Heat transfer
Dipprey and Sabersky [33] (1963)	Granular roughed $0.0024 \leqslant e/d_i \leqslant 0.049$ Water	$1.20 \leqslant Pr \leqslant 5.94$ Pr=1.2: $6\times10^4 \leqslant Re \leqslant 5\times10^5$ Pr = 5.94: $1.4\times10^4 \leqslant Re \leqslant 1.2\times10^5$ Deviation: ± 10%	$f = 2\left[2.5\ln(d_i/2e) - 3.75 + \overline{B}(e^+)\right]^{-2}$ $e^+ = (e/d_i)Re\sqrt{f/2}$ $\overline{B}(e^+)$: Friction similarity function	$Nu = \frac{(f/2)RePr}{1+\sqrt{f/2}[\overline{g}(e^+)Pr^n - \overline{B}(e^+)]}$ $\overline{g}(e^+)$: Heat transfer similarity function
Webb et al. [26] (1971)	Repeated transverse ribs: $0.01 \leqslant e/d_i \leqslant 0.04$ $10 \leqslant p/e \leqslant 40$ Air, Water, n-butyl alcohol	e^+>35 $6000 \leqslant Re \leqslant 100000$. $0.71 \leqslant Pr \leqslant 37.6$ Deviation: ± 11%	$f = 2[2.5\ln(d_i/2e) + 0.95(p/e)^{0.53} - 3.75]^{-2}$ $e^+ = (e/d_i)Re\sqrt{f/2}$	$Nu = \frac{(f/2)RePr}{1+\sqrt{f/2}[4.5(e^+)^{0.28}Pr^{0.57} - 0.95(p/e)^{0.53}]}$
Han et al. [34] (1978)	Repeated transverse ribs $5 \leqslant p/e \leqslant 20$, $0.032 \leqslant e/d_h \leqslant 0.102$, β: 20°–90° e/w:0.67-1 Air	$7.5\times10^4 \leqslant Re \leqslant 2\times10^5$ Deviation: within ± 40%	$f = 2(Re^+ - 2.5\ln(2e/d_h) - 3.75)^{-2}$ $Re^+ = 4.9(e^+/35)^m/[(\alpha/90^\circ)^{0.35}(10/P/e)^n \times (\beta/45)^{0.57}$ If $e^+ < 35, m = -0.4$; If $e^+ \geqslant 35, m = 0$; If $P/e < 10, n = -0.13$; If $P/e \geqslant 10, n = 0.53(\beta/90^\circ)^{0.71}$	$Nu = \frac{fRePr}{[He^+ - Re^+](2f)^{1/2}+2}$ $He^+ = 10(e^+/35)^i/(\alpha/45^\circ)^j$ $i = 0, when\ e^+ < 35; i = 0.28,$ when $e^+ \geqslant 35$; $j = 0.5,$ when $\beta < 45^\circ$; $j = -0.45,$ when $\beta \geqslant 45^\circ$;
Carnavos [37] (1980)	Helical and longitudinal ribs. d_i:8–22.2 mm, N_s:6–38 e:0.6–2 mm, α:0-30°, δ_t:0.26–0.8 mm. air, water, and ethylene glycol-water	$1\times10^4 \leqslant Re \leqslant 10^5$ $0.7 \leqslant Pr \leqslant 30$ Deviation: within ± 10%	$f = 0.046Re^{-0.2}(F^+)^{-1}$ $F = (A_{fa}/A_{fn})^{0.5}(\sec\alpha)^{0.75}$	$Nu = 0.023Re^{0.8}Pr^{0.4}(F)$ $F = (A_{fa}/A_{fc})^{0.1}(A_n/A_a)^{0.5}(\sec\alpha)^3$
Kader and Yaglom [41] (1977)	Repeated transverse ribs e^+:10–4000 $4 \leqslant p/e \leqslant 40$,	$0.7 \leqslant Pr \leqslant 4585$ $3\times10^4 \leqslant Re \leqslant 2\times10^5$ Agree satisfactorily with experiment result	$f = \frac{\Delta P d_i}{2Lpv^2}$	$Nu = \frac{1.42(f/2)^{0.5}RePr}{5(e^+)^{0.25} - 3\ln(e/d_i) + 5.6 - 4.5/(1-e/d_i)^2 + 9.5(f/2)^{0.5}}$
GEE and Webb [35] (1980)	Transverse and helical ribs α: 30°, 49°, 70°, p/e = 15 Air	$6\times10^3 \leqslant Re \leqslant 6.5\times10^4$ Pr = 0.71 Compared with literature	$f = 2\left[\overline{B}(e^+,\alpha)/(\alpha/50)^{0.16} - 2.5\ln(2e/d_i) - 3.75\right]^{-2}$ $\overline{B}(e^+,\alpha)$: Friction similarity function	$Nu = \frac{(f/2)^{0.5}RePr}{1+\sqrt{f/2}[\overline{g}(e^+,Pr,\alpha)/(\alpha/50)^j - \overline{B}(e^+,\alpha)]}$ $j = 0.37$ for $\alpha < 50^\circ$; $j = -0.16$ for $\alpha > 50^\circ$ $\overline{g}(e^+,Pr,\alpha)$: Heat transfer similarity function
Wang *et al.* [36] (1996)	Helical fin d_o : 7.00 – 9.52 mm d_i : 6.46 – 8.96 mm e : 0.15 – 0.2 mm α : 17 – 25° δ_t : 0.26 – 0.8 mm Water	$2.5\times10^3 \leqslant Re \leqslant 4\times10^4$ Pr = 5.38,7.33 Deviation: f: 95.8% within ± 10%. Nu: 85.2%within ± 10%.	$f = 2(\frac{d_i e^+}{e})^2 Re^{-2}$ $e^+ = 0.1407 + 0.093675X_f + 0.58464/\ln(X_f)$ For $e^+ \leqslant 23$ $e^+ = 0.07313 + 0.09571X_f$ For $e^+ \geqslant 23$ $X_f = Re\left(\frac{e}{d_i+0.005}\right)\frac{Ns^{0.25}}{(\cos\alpha)^{0.5}}$	$Nu = \frac{fRePr}{2(1+\sqrt{f/2}[\overline{g}(e^+)Pr^n - B(e^+)])}$ $B(e^+) = \exp(y_b)X_b$, $y_b = 2.45805 - 0.987261ne^+$ $X_b = Re(\frac{e}{d_i})\frac{\cos\alpha z}{n_f^{0.7}}$, $B(e^+) = y_g Xg$, $Xb = \frac{n_f(tg\alpha)^{0.1}}{(e/d_i)^{0.4}}$ $y_g = 0.007705 + 0.321(\ln e^+)/e^+$ For $e^+ \leqslant 23$ $y_g = 0.06501 - 0.51903/e^+ + 5.5956/(e^+)^2$ For $e^+ \geqslant 23$
Ravigururajan and Bergles [27] (1996)	e/d_i : 0.01 – 0.1 p/d_i : 0.1 – 1.0 α/90 : 0 – 1.0	10,000 < Re < 100,000 $0.7 \leqslant Pr \leqslant 35$ Deviation:f: 77% of data(1658 points) within ± 20%. Nu: 69% of data (18070 points) within ± 20%.	$f/f_p = 0.25 \times \left\{1 + [29.1Re^{(0.67-0.06p/d-0.49\alpha/90)} \times (e/d)^{(1.37-0.157p/d)} \times (p/d)^{(-1.66Re\times10^{-6}-0.15p/d)} \times (1 + 2.94\sin(45/Ns))]^{15/16}\right\}^{16/15}$	$Nu/Nu_p = \left\{1 + [2.64Re^{0.036}(e/d)^{0.212} \times (p/d)^{-0.21} \times (\alpha/90)^{0.29}(Pr)^{0.024}]^7\right\}^{1/7}$

(*continued on next page*)

Table 1 (*continued*)

Authors	Tube geometry/Fluid	Validation range	Friction	Heat transfer
Jensen and Vlakancic [29] (1999)	Helical fins d_o : 24.30 – 26.57 mm d_i : 21.18 – 24.41 mm N_s : 8 – 54 e : 0.18 – 2.06 mm α : 0 – 45° s : 0.4 – 1.84 mm Water, ethylene glycol	2,500 < Re < 70,000 Deviation: generally within ± 15% Also compared with other published data	$f/f_p = \left(\frac{l_{spc}}{d_i}\right)^{-1.25}\left(\frac{A_n}{A_o}\right)^{1.75}$ High finned tubes(Re ⩾ 5000): $\frac{l_{spc}}{D_i} = \frac{1}{d_i}[1 - 0.203(SW)^{0.65}(H)^{0.20}]$ Micro finned tubes(Re ⩾ 20000): $\frac{l_{spc}}{d_i} = [1 - A(SW)^b(H)^c(W)^d]$ For $H \leqslant 0.04$: $A = 1.577$, $b = 0.64$, $c = 0.53$, $d = 0.28$ For $0.04 \leqslant H \leqslant 0.06$, $A = 0.994$, $b = 0.89$, $c = 0.44$, d=0.41 Micro finned tubes(2500 ⩽ Re ⩽ 20000): $\frac{l_p}{d_i} = \frac{A_{fc}}{A_{fn}}(1 - H) + \frac{A_{fm}}{A_{fn}}\frac{\pi}{N}\left(1 - \frac{H}{2}\right) - \frac{s}{d_i}$	$Nu/Nu_p = \left(\frac{l_p}{D_i}\right)^{-1/2}\left(\frac{A_n}{A_o}\right)f(\text{geometry})(\text{Re} \geqslant 4,000)$ High finned tubes $f(\text{geometry}) = (A_a/A_n)^{0.29}[1 - 1.792(SW)^{0.64}(H)^{2.76}(Re)^{0.27}]$ Micro finned tubes $f(\text{geometry}) = (A_a/A_n)^{1.0}[1 - 0.059(SW)^{-0.31}(W)^{-0.66}]$
Webb *et al.* [38] (2000)	Helical ribs, e/d_i:0.024–0.041 p/e : 2.39 – 12.84 α : 25 – 45° θ : 41° t_t/d_i = 0.015 Water	5.08 ⩽ Pr ⩽ 6.29 20,000 < Re < 80,000. f: within an error of ± 30% *Nu*: ± 10%, also compared with other published data	$f = 0.108\text{Re}^{-0.283}Ns^{0.221}(e/D_i)^{0.785}\alpha^{0.78}$	$Nu = 0.00933\text{Re}^{0.819}Ns^{0.285}(e/D_i)^{0.323}\alpha^{0.505}\text{Pr}^{1/3}$
Ji *et al.* [40] (2012)	$1 \leqslant Ns \leqslant 45$, $0.016 \leqslant e/d_i \leqslant 0.04$, $13 \leqslant \alpha \leqslant 45$	10,000 ⩽ Re ⩽ 100,000 4.98 ⩽ Pr ⩽ 8.22 *Nu*: 89% of data (288points) within ± 20%	$f = \frac{\Delta P d_i}{2L\rho v^2}$ determined by experiment	$Nu = \frac{(f/8)(\text{Re}-1000)\text{Pr}}{1+12.7(f/8)^{1/2}(\text{Pr}^{2/3}-1)}\left[1 + \left(\frac{d_i}{L}\right)^{2/3}\right]\left(\frac{\text{Pr}}{\text{Pr}_w}\right)^{0.11}$

the internally grooved tubes. For all the 152 data in the experiment of 16 tubes, most of the relative deviation was within ± 10%. It was also compared with other data available in the literature, and the deviation of more than 93% of data was within ± 20%, 99% within ± 40%. Since the microscopic parameters of internally finned tube was not easily to be determined and friction factor is easy to be tested with experiments for internally finned tubes, the proposed equation was practically applicable and its accuracy was also acceptable for engineering design without the detailed geometric information.

Figure 3 is the comparisons of the prediction models and experimental results in Webb et al. [38]. Internal fin height and number of fins are 0.493 mm and 25 respectively. The helix angle of fin is 35°. It is found that the models of Ravigururajan and Bergles [27] (1996), and Webb et al. [38] (2000) based on the geometry of fin, over-predicts the experimental results within 7.0%–16.6% and 1.5–2.8%, respectively. The predictions deviations of Ji et al. [40] (2012) are approximately within ± 12%. Under-predictions in a range of 30.9% to 34.0% are observed with Jensen and Vlakancic model [29] (1999). The deviations of Webb [26], Kader and Yaglom [41], and Carnavos [37] models are generally in the range of ± 60%.

2.3. Experimental results of internally finned tube

Although all the aforementioned correlations are based on test data, for a comprehensive review and performance comparison of enhanced techniques the original test data are of more importance. To the best of the authors' knowledge, they are collected as follows.

First it should be noted that more than 90% of experimental data of plain tube in the survey agree with Dittus–Boelter and Fanning equations with the deviations of ±20% depending on the literature:

$$\text{Dittus} - \text{Boelter equation}: \quad Nu = 0.023\text{Re}^{0.8}\text{Pr}^{n} \tag{3}$$

$$\text{Fanning equation}: \quad f = 0.079\text{Re}^{-1/4} \tag{4}$$

Thus it can be confirmed that the following comparisons are based on the same references.

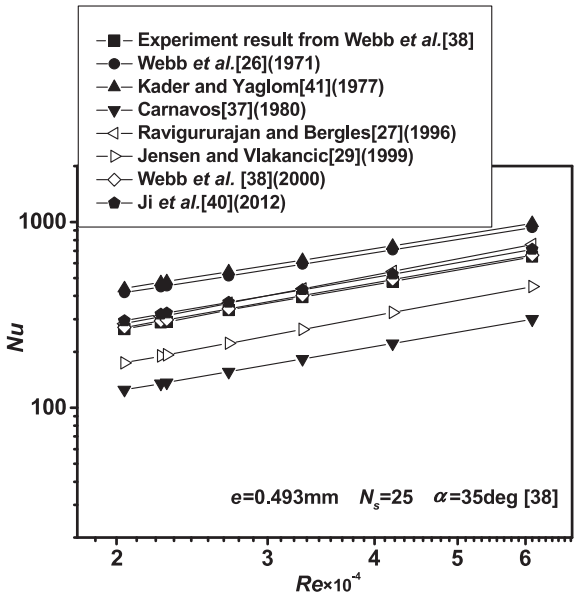

Fig. 3. Comparisons the prediction models and experimental result in Webb et al. [38].

Table 2
Experimental data of internally finned tubes.

Researcher	Re	Fluid	Tube/ number	Best tube/feature	f/f_r	Nu/Nu_r
Wang et al. [36] (1996)	$2.5–40 \times 10^3$	Water	Micro-fin/7	e/d_i = 0.022, Ns = 60 p/e = 7.22, α = 18°, d_i = 8.96 mm	1.5–2.2	0.8–2.1
Brognaux et al. [42] (1997)	$2.5–50 \times 10^3$	Water	Micro-fin/6	e/d_i = 0.036, Ns = 78 p/e = 1.66, α = 20°, d_i = 14.57 mm	1.1–1.7	1.6–1.8
Jensen and Vlakancic [29] (1999)	$13–70 \times 10^3$	Water, EG	Micro-fin/8 Highfin/7	e/d_i = 0.014, Ns = 54 α = 45°, s = 0.9 mm, d_i = 24.41 mm	2.1–2.4	3.0–3.7
Al-Fahed et al. [1](1999)	$0.25–2.5 \times 10^3$	Oil	Micro-fin with inserts/7	y = 3.6, w = 13.2 e/d_i = 0.014, Ns = 60 α = 15°, d_i = 14.0 mm	2.7–8.9	1.8–3.2
Webb et al. [38] (2000)	$20–60 \times 10^3$	Water	Micro-fin/7	e/d_i = 0.021, Ns = 45 p/e = 2.81, α = 45°, d_i = 15.54 mm	2.1–2.4	2.2–2.3
Copetti et al. [43] (2004)	$0–20 \times 10^3$	Water	Micro-fin/1	e/d_i = 0.022, Ns = 60 p/e = 2.34, α = 18°, d_i = 8.95 mm, s = 0.29 mm	0.9–1.9	0.8–2.8
Han&Lee [44] (2005)	$3–40 \times 10^3$	Water	Micro-fin/4	e/d_i = 0.013, Ns = 60 p/e = 8.33, α = 25°, d_i = 8.92 mm	Up to 2.4	1.0–1.6
Naphon and Sriromruln [45] (2006)	$8–16 \times 10^3$	Water	Micro-fin/1	e/d_i = 0.022, Ns = 60 d_i = 8.92 mm	1.6–2.0	1.0–1.3
Li et al. [20] (2007)	$2.5–90 \times 10^3$	Water, oil	Micro-fin/1	e/d_i = 0.017, Ns = 82 p/e = 2.23, α = 25.5° θ = 66.5°, d_i = 17.5 mm	1–1.5	1–2.0
Siddique and Alhazmy [46] (2008)	$3.3–22.5 \times 10^3$	Water	Micro-fin/1	e/d_i = 0.027, Ns = 50 α = 18°, d_i = 7.38 mm	1.6–2.0	1.0–2.1
Zdaniuk et al. [30] (2008)	$12–60 \times 10^3$	Water	Micro-fin/8	e/d_i = 0.024, Ns = 45 α = 48°, d_i = 15.58 mm	2.8–3.2	2.0–2.4
Nagarajan et al. [47] (2010)	$6–1.2 \times 10^3$	Water	Micro-fin with inserts/6	L-R/y = 7.44 Ns = 75, α = 18°, d_i = 12.09 mm	5.2–6.8	2.5–3.3
Ji et al. [40] (2012)	$10–100 \times 10^3$	Water	Micro-fin/16	e/d_i = 0.021, Ns = 45 α = 40°, d_i = 16.61 mm	2.9–3.2	2.9
Eiamsa-ard& Wongcharee [48] (2012)	$5.65–17 \times 10^3$	Water/ CuO nano fluid	Micro-fin with inserts/3	MF-DT y = 3 e/d_i = 0.020, α = 25° p/e = 2.82, d_i = 8.64 mm	12.7–13.5	3.6–5.1
Eiamsa-ard and Wongcharee [49] (2013)	$5 .65–17 \times 10^3$	Water	Micro-fin with inserts/6	MF-CDT, y = 3 e/d_i = 0.019, Ns = 60 α = 25°, d_i = 8.64 mm	12.0–12.2	3.5–4.7
Filho and Jabardo [50] (2014)	$5–50 \times 10^3$	R134a, R22	Micro-fin/3	Herringbone, α = 18° e/d_i = 0.022, Ns = 70, θ = 33°, d_i = 8.92 mm	2.5–2.9	1.2–2.3

*f_r and Nu_r are calculated from Blasius and Dittus–Boelter equation, respectively.

The experimental system usually include a closed liquid loop. The loop consists a pump, liquid storage tank, flow meter, temperature and pressure drop transducers. The liquid temperature and stability can be precisely controlled before entering the test section. The system also include the liquid heating or cooling system for the test section. The experimental apparatus for other enhanced techniques in this paper are similar.

Experimental studies of internally-finned tube with different geometrical parameters reported in the literature are summarized in Table 2. The tube which yields the best heat transfer performance among those studied are presented. Reynolds number in the research was in the range of 2500–100,000, mostly in the turbulent flow region. Test fluids include water, air, oil, refrigerant, and nanofluids, with most data being of water.

As shown in Table 2, the largest heat transfer enhancement ratio of the internally micro-finned tube is 2.9 compared with smooth tube, and that of friction factor is 3.2. The largest enhancement ratios of heat transfer and friction factors are roughly the same for the internally finned tubes.

For the 13 internally finned tubes published since 1996 their heat transfer characteristics vs. Reynolds number are compared in Fig. 4 where Nu/Pr^n and Reynolds number, Re, are taken as the ordinate and abscissa, respectively. The value of n is 0.4 for heating and 0.3 for cooling or indicated by the author. The Reynolds number range is from 3×10^3 to 100×10^3. Dittus–Boelter equation for plain tube is also presented in Fig. 4 for comparison, where the curves designated by 1×, 2×, 4×, and 6 × show the enhancement ratio over the value predicted by the D-B equation. As shown in the figure, the enhanced ratios of most tubes are in the range of 2–4. The enhanced ratio decreases for some tubes at lower Re region, while three structures have higher ratios. The three structures are microfin with inserts, and their increased ratios of friction factor are much higher as it will be seen later.

The friction factors are shown in Fig. 5. Those curves designated by 1×, 2×, 4×, and 13 × show the increase ratios over the value predicted by Fanning equation. The ratios of friction factor for most internally finned tubes are from 1 to 4 compared with smooth tube, generally consistent with heat transfer enhancement ratios.

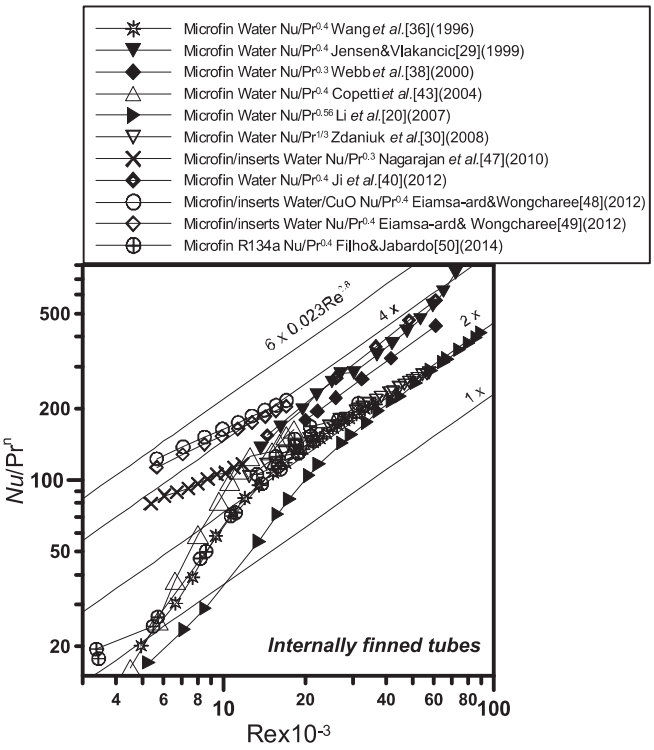

Fig. 4. Experimental result of Nu/Pr^n versus Re for internally finned tubes.

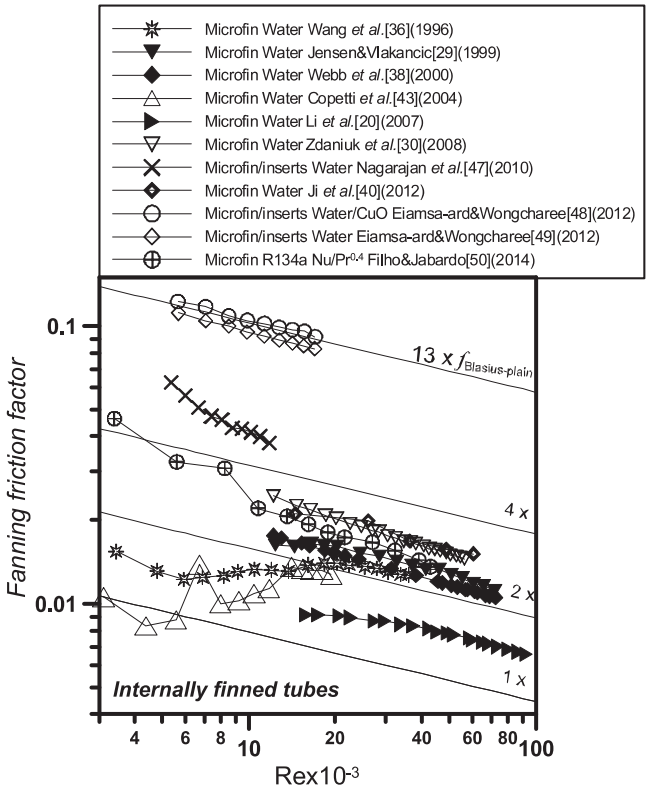

Fig. 5. Experimental result of Fanning friction factor versus Re for internally finned tubes.

Among all the internally finned tubes, the friction factors of the three tubes with inserted helical tapes are at the highest level. The friction factors of two such structures are as much as 13 times higher over plain tube. However, as can be seen in Fig. 4 only up to 500% increase of internal heat transfer coefficient can be obtained.

2.4. Hydraulic-thermal performance evaluation of internally finned tube

Come here the performance evaluation of the aforementioned enhanced tubes are conducted by using the plot proposed by Fan et al. [17].The reference values of heat transfer and friction factor for the plain tube are determined by Dittus–Boelter equation and Blasius equation, respectively. It should be noted that the comparison and evaluation for enhanced tube and plain tube is based on the same internal diameter (d_i). For internally finned tube, internal diameter is the root diameter of the internal fins.

In Fig. 6, experimental data for the internally finned tubes are presented in the performance evaluation plot. Region 1 is featured by enhanced heat transfer without energy-saving. The heat transfer is deteriorated compared with the plain tube per identical pumping power; In Region 2, the heat transfer can be enhanced with identical pump power consumption. In Region 3 heat transfer is enhanced per identical pressure drop, and Region 4 is the most favorable, where heat transfer enhancement is obtained under the identical flow rate. It is important to note that at the equal ratio of f_e/f_r, the higher the heat transfer enhanced ratio, the more difficult to accomplish the technique. As shown in Fig. 6, the data for internal integrally-finned tubes without inserts mainly locate in Regions 4 except the tubes investigated in [20,30,36,50]. For internally finned tubes with helical tape inserts, friction factor enhanced ratio is significantly increased. Hence their data are mainly in Region 3, where heat transfer can be enhanced with the same pressure drop penalties for driving heat transfer medium. More attention needs to be paid for four special data in Fig. 6. There are three black triangles located in the fourth quadrant where heat transfer is deteriorated but pressure drop is increased. These situation should be avoided for any practical application. On the other

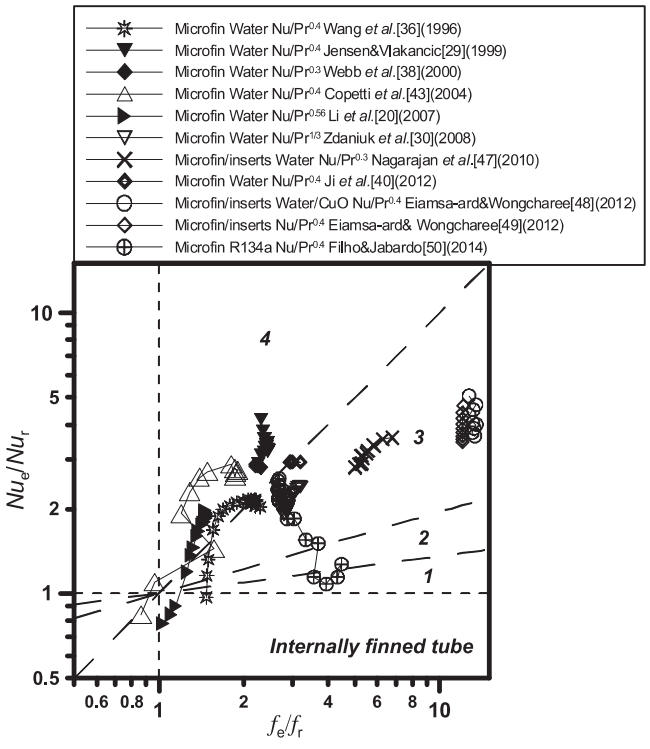

Fig. 6. Performance evaluation plot for internally finned tubes.

hand, one white triangle locates in the 3rd quadrant, where both heat transfer and pressure drop decrease compared with the referenced one. For this case if the reduction of friction factor is much larger than the reduction of heat transfer, the related structure may still be useful for enhancing heat transfer in the sense of that per identical pressure fluid drop the heat transfer rate may be increased.

By using the new performance evaluation plot, both heat transfer and flow friction are considered, the internal integrally-finned tubes in the investigations of Jensen and Vlakancic [29] and Copetti et al. [43] are the best performed tubes in the comparison. The geometries of micro-fin tubes are characterized by $e/d_i = 0.014$, $Ns = 54$, $\alpha = 45°$, $s = 0.9$ mm, and $d_i = 24.41$ mm in [29]; and $e/d_i = 0.022$, $Ns = 60$, $p/e = 2.34$, $\alpha = 18°$, and $d_i = 8.95$ mm [43]. The performance is worse for the tube in the investigation of Filho and Jabardo [50].

3. Twisted tape and coil inserts

3.1. Introduction of pipe with twisted tape and coil inserts

Twisted-tape inserts have been widely used in improving the heat transfer of both laminar and turbulent flow. The pipe with internal twisted tape is accomplished by twisting a metallic strip and inserting the tape into a tube. The tapes can promote the transverse mixing and produce swirl flow or vortex inside the tube, thus producing a sizable augmentation for internal single phase convection heat transfer. Tape inserts are cost-competitive and can easily be installed in an existing plain tube heat exchanger. The drawbacks of internally twisted tape are that the tape is difficult to fix at a constant position inside the pipe and it is easy to be fouled. The wire coil insert has the similar features with tape.

There have been many investigations on the heat transfer and pressure drop characteristics of single-phase heat transfer in tape-generated swirl flow since 1921 [51]. The twisted tape can either be tight or loose [52], roughed [53], partial [54] or full length, single or double [55], inside smooth or internally finned tubes [56,57]. The tight bounding of tapes has the effect of integral fin, which is desirable for heat transfer enhancement. This favorable effect for loose tape might be negligible. However, loose tape with partial length can remove the fouling inside the tube surface. For the tape roughed with ribs or three dimensional protrusions, additional turbulence around the tape surface can also be quite beneficial to heat transfer enhancement. As indicated in previous section, helical-ribbed tube with twisted tapes also shows a considerable improvement of heat transfer compared with helical-ribbed tube acting alone in the low Reynolds number region.

The velocity distribution in a tube fitted with twisted tapes is very complicated. Experimental results in [58,59] indicated that the axial velocity is nearly constant over most of cross section and characterized by a helicoidal distribution. The profile of axial velocity appears to be tangent at every point to a helix. The flows with swirl will result in a forced vortex in the tube cross-section plane. This helical core flow is broken down at the tube walls, where boundary layer effects should predominate. Boundary-layer flows along the tube surface and tapes may also be sucked into the main stream moving along the tube axis. The interactions of core flow, tube blockage, vortex, and swirl motion result in both increased friction losses and heat transfer for twisted tape inserts. In general, the mechanisms of heat transfer enhancement is attributed to the following aspects: swirl flow mixing, increased flow velocity and flow length, and favorable fin effects [60]. As the hydraulic characteristics are concerned the major drawback of inserted tapes is the pretty high pressure drop [56].

As shown in Fig. 7, geometric features of the internally twisted tapes include: 180° twist pitch, H; tape width, w; tape thickness, δ; and inner diameter of tubes, d_i. Twist ratio is $y = H/w$. The lower limit of twist ratio is described by $y = \infty$, or a straight tape insert that divides the flow inside tube into two circular segments. Experimental results show that the twist ratio is the major factor affecting heat transfer enhancement.

3.2. Heat transfer and friction correlations for tube with insertion of twisted tape

One of the early analytical predictions was made by Smithberg and Landis [58]. The available experimental correlations of friction factor and Nussult number are shown in Table 3. The correlation of Hong and Bergles [61] was probably the first experimentally based correlations to predict the laminar heat transfer coefficient of twisted tape inserts. The standard deviation of the correlation from experimental data was within 16.4 percent. This correlation was also in fair agreement with limited numerical and analytical predictions [62,63].

In order to develop a more generalized correlations, Manglik and Bergles [59,60] analyzed the experimental data of f and Nu for water and ethylene glycol, twisted-tape inserts having $y = 3.0$, 4.5, and 6.0. The data for gas and water reported in the literature were also considered. For laminar flow, swirl parameter, $Sw = \mathrm{Re}/\sqrt{y}$ was introduced to describe tape-induced swirl flows. Buoyancy-driven free convection effects were also taking into account. These parameters along with numerical solutions for flows in circular-segment ducts are incorporated in correlations. Over a broad range of tape geometry and fluid flow conditions, the correlations predicted the experimental data and those reported in the literature very well. For transition and turbulent flow, the correlation was based on the case of straight tape inserts ($y = \infty$). Tape twist effects are modeled by functional relationships with the form $(f/f_{y=\infty})$ and $(Nu/Nu_{y=\infty})$. The empirical correlations of Naphon [64] and Bas and Ozceyhan [65] (2012) were based on experimental data.

It should be noted that although considerable investigations have been made on the tube fitted with twisted tapes, there are still great relevant disagreements on the correlations of frictions and heat transfer. The general applicability of the correlations is still limited. It might be due to the complexity of the induced fluid flow and installation method of twisted tapes. As in the process of insertion, the tightness of bonding is a crucial factor: a small range of variance may cause a significant discrepancy in test data.

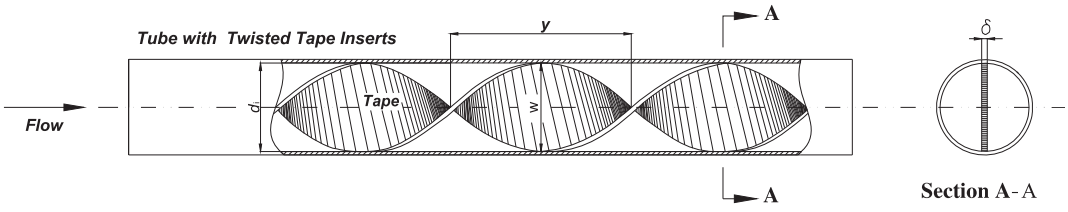

Fig. 7. Illustration of tubes with internal twisted tapes.

Table 3
Heat transfer and friction correlations for tube inserted with twisted tapes.

Authors	Tube geometry	Validation range	Friction	Heat transfer
Smithberg and Landis [58] (1964)	Twisted-tape inserts Twist ratio: y:3.62–22 Air, water Units used in this paper is: ft, Btu, hr, F	0.7. $\leqslant$ Pr $\leqslant$ 10 2000 $\leqslant$ Re $\leqslant 10^5$ Deviation: *f*: ± 10% *Nu*: ± 20%	$f=\left[0.046+2.1\left(\frac{H}{d_i}-0.5\right)^{-1.2}\right]Re^{-n}$ $n=0.2\left[1+1.7\left(\frac{H}{d_i}\right)^{-1/2}\right]$	$Nu=\frac{(1+2\eta_e/\pi)\mathrm{RePr}}{1+\frac{700}{\mathrm{Re}f}\left(\frac{d_i}{H}\right)\left(\frac{d_h}{d_i}\right)\mathrm{Pr}^{0.731}}\left[\frac{50.9(d_i/H)}{\mathrm{Re}\sqrt{f}}+0.023\left(\frac{d_i}{d_h}\right)Re^{-0.2}\mathrm{Pr}^{-2/3}\left(1+\frac{0.0219}{\left(\frac{H}{d_i}\right)^2 f}\right)^{1/2}\right]$ $\eta_e=\frac{\eta_f}{1+\eta_f\frac{Pd_i}{\gamma f^3}}$ $\eta_f=\frac{Q}{hA_{fin}(T_w-T_f)}$ A_{fin} wetted surface area
Hong and Bergles [61] (1976)	Twisted-tape inserts Twist ratio: y = 2.45, 5.08 Water, EG	Water: 3 $\leqslant$ Pr $\leqslant$ 7 83 $\leqslant$ $\mathrm{Re}_s\leqslant$2460 EG:84 $\leqslant$ Pr $\leqslant$ 192,13 $\leqslant$ Re $\leqslant$ 390 Fair agreement with the analytical predictions given in references		$Nu=5.172[1+5.484\times10^{-3}\mathrm{Pr}^{0.7}(Re/y)^{1.25}]^{0.5}$ $y=H/d_i$
Shah and London [54] (1978)			$f_i=46.45/Re_i$ $\mathrm{Re}_i/y\leqslant6.7$ $f_i=42.24/Re_i^{0.95}y^{0.05}$ $6.7\leqslant\mathrm{Re}_i/y\leqslant100$ $f_i=1.1C(Re_i/y)^{0.3}\mathrm{Re}_i$ $100\leqslant\mathrm{Re}_i/y$	$Nu_i=5.172[1+5.4838\times10^{-3}\mathrm{Pr}^{0.7}(Re_s/y)^{1.25}]^{0.5}$ $C=8.8201y-2.1193y^2+0.2108y^3-0.0069y^4$
Saha et al. [54] (1990)	Twisted-tape inserts connected by thin circular rods 2.5 $\leqslant s\leqslant$ 10 Water	5000 < Re < 43,000 4 $\leqslant$ Pr $\leqslant$ 5.5 Deviation: *f*: 94% of experimental data within ± 20% *Nu*: all within ± 20%	$f=38.4\zeta_1\mathrm{Re}_i^{-0.95}y^{-0.05}(1+Cs)$ $6.7\leqslant\mathrm{Re}/y\leqslant100$ $f=0.5(38.4\zeta_1\mathrm{Re}^{-0.95}y^{-0.05}+C_1\zeta_1\mathrm{Re}^{-0.07}y^{-0.3})(1+Cs)$ $100\leqslant\mathrm{Re}/y\leqslant155$ $f=C_1\zeta_1\mathrm{Re}^{-0.7}y^{-0.3}(1+Cs)$, $155\leqslant\mathrm{Re}/y$ ζ_1, C and C_1, were given in Ref. [54]	$Nu=5.172[1+6.7482\times10^{-3}\mathrm{Pr}^{0.7}(K_1\mathrm{Re}/y)^{1.25}]^{0.5}(1+Cs)X$ K_1, C and X, were given in Ref. [54]
Manglik and Bergles [60] (1993)	Twisted-tape inserts y = 3.0, 4.5, and 6.0 Water (3.5 < Pr < 6.5) and EG (68 < Pr < 100)	300 < Re < 30,000 *f*: ± 10 percent *Nu*: ± 15 percent of the experimental data	$f=15.767\left(\frac{\pi+2-2\delta/d_i}{\pi-4\delta/d_i}\right)^2(1+10^{-6}Sw^{2.55})^{1/6}/\mathrm{Re}$ $Sw=\mathrm{Re}/\sqrt{y}\left(\frac{\pi}{\pi-4\delta/d_i}\right)(1+(\pi/2y)^2)^{1/2}$	$Nu_i=4.612\left\{\left[\left(1+0.0951\,\mathrm{Gz}^{0.894}\right)^{2.5}+6.413\times10^{-9}(Sw\cdot\mathrm{Pr}^{0.391})^{3.835}\right]^{2.0}+2.132\times10^{-14}(\mathrm{Re}_{ax}\cdot Ra)^{2.23}\right\}^{0.1}\left(\frac{\mu_f}{\mu_w}\right)^{0.14}$
Manglik and Bergles [59] (1993)	Twisted-tape inserts *y* = 3.0, 4.5, and 6.0 Water and ethylene glycol	Re > 10^4 *f* and *Nu*: excellent agreement with experimental data, and those reported in the literature for gases and liquids	$f=0.0791\left(\frac{\pi}{\pi-4\delta/d_i}\right)^{1.75}\left(\frac{\pi+2-2\delta/d_i}{\pi-4\delta/d_i}\right)^{1.25}\cdot(1+2.752/y^{1.29})/\mathrm{Re}^{0.25}$ For straight tape inserts, $y=\infty$	$Nu_i=[1+0.769/y]Nu_{y=\infty}$ $Nu_{y=\infty}=0.023\mathrm{Re}^{0.8}\mathrm{Pr}^{0.4}(\frac{\pi}{\pi-4\delta/d_i})^{0.8}\left(\frac{\pi+2-2\delta/d_i}{\pi-4\delta/d_i}\right)^{0.2}\phi$, $\phi=\left(\frac{\mu_f}{\mu_w}\right)^n$ or $\left(\frac{T_f}{T_w}\right)^m$ n = 0.18 for liquid heating and 0.30 for liquid cooling m = 0.45 for gas heating and 0.15 for gas cooling
Naphon [64] (2006)	Twisted-tape inserts Water, Pr > 3 3.1 $\leqslant$ y $\leqslant$ 5.5	7000 $\leqslant$ Re $\leqslant$ 23,000 Majority of present data, *Nu* within ± 15%, *f* within ± 10%	$f=3.517\mathrm{Re}^{-0.414}(1+1/y)^{1.045}$	$Nu=0.648\mathrm{Re}^{0.36}(y)^{0.443989}(1+1/y)^{2.475}\ \mathrm{Pr}^{1/3}$
Bas and Ozceyhan [65] (2012)	Twisted tape inserts Water, y = 2, 2.5, 3, 3.5 and 4; clearance ratios c/*w* = 0.0178, 0.0357	5132 < Re < 24,989 Experiment based correlations	$f=6.544291\mathrm{Re}^{-0.452085}(y)^{-0.730772}\ (\mathrm{c}/w)^{-0.1579}$	$Nu=0.406903\mathrm{Re}^{0.586556}(y)^{0.443989}(\mathrm{c}/w)^{0.055072}\ \mathrm{Pr}^{0.38}$

Table 4
Experimental data for the tubes with twisted tape and coil inserts.

Researcher	Re	Fluid	Tube/ number	Best tube /feature	f/f_r	Nu/Nu_r
Smithberg and Landis [58] (1964)	$5–50 \times 10^3$	Air, water	Twisted tape/5	y = 3.62, c = 0.127 mm d_i = 35.1 mm	2.2–2.7	2.3–2.7
Lopina and Bergles. [51] (1969)	$8–130 \times 10^3$	Water	Twisted tape/5	y = 2.48, δ = 0.343 mm, d_i = 4.91 mm	3.4–3.7	1.7–1.9
Bergles et al. [56] (1969)	$13–70 \times 10^3$	Water	Twisted tapes in roughed tube/3	y = 2.55, δ = 0.472 mm, d_i = 6.35 mm	4.9–7.0	1.6–2.0
Uttarwar and Raja Rao [66] (1985)	40–620	Oil	Wire coil inserts/7	p/d_i = 0.4 e/d_i = 0.079, α = 76° d_i = 25.2 mm	1.9–4.1	3.8–5.4
Saha et al. [54] (1990)	$5–43 \times 10^3$	Water	Twisted tape/16	y = 10, space ratio = 2.5, δ = 0.4 mm, d_i = 13.0 mm	2.9–3.6	1.2–3.6
Prasad and Shen [67] (1993)	$35–92 \times 10^3$	Water	Wire coil inserts/4	p/d_i = 0.201, e/d_i = 0.058, d_i = 14.0 mm	17.5–22.4	1.7–2.2
Chakroun and Al-Fahed [52] (1996)	$0.23–2.3 \times 10^3$	Oil	Twisted tape /15	y = 3.6, δ = 0.5 mm, c = 0.8 mm, d_i = 14 mm	3.4–7.6	1.3–3.2
Al-Fahed et al. [1] (1999)	$0.35–3.6 \times 10^3$	Oil	Twisted tape in finned tubes /7	y = 3.6, δ = 0.5 mm, c = 0.8 mm, e/d_i = 0.014, Ns = 60, α = 15°, d_i = 14.0 mm	3.5–8.7	1.3–3.2
Liao and Xin [57] (2000)	$16–48 \times 10^3$	Water, EG, oil	Twisted-tape in roughed tubes/12	p/d_i = 5, e/d_i = 0.077, δ = 0.5mm, d_i = 13.5 mm	6.4–7.1	1.6–2.2
Zimparov[68] (2001)	$3–60 \times 10^3$	Water	Twisted-tape in corrugated tubes / 12	y = 4.7, δ = 0.8 mm, p/e = 7.45, α = 68°, e/d_i = 0.0569, d_i = 13.73 mm	14.0–17.1	0.7–7.4
Zimparov [69] (2002)	$4–60 \times 10^3$	Water	Twisted-tape in corrugated tubes / 12	y = 2.4, δ = 0.8 mm, p/e = 13.48, α = 82.2°, e/d_i = 0.044, d_i = 13.65 mm	9.8–11.9	4.3–7.6
Sivashanmugam and Suresh [70] (2007)	$0.23–2.7 \times 10^3$	Water	Twisted tape /16	y = 2.93, w = 8.5 mm d_i = 25.45 mm	4.7–7.0	2.7–4.1
Chang et al. [53] (2007)	$5–25 \times 10^3$	Water	Serrated twisted tape/8	y = 1.56, δ = 1.5 mm, w = 15 mm, d_i = 15 mm	48.7–79.8	3.7–4.8
Bharadwaj et al. [2] (2009)	$0.2–30 \times 10^3$	Water	Twisted tape in finned tubes /6	y = 3.33, e/d_i = 0.021, Ns = 75, α = 23°, d_i = 14.8 mm	12.0–12.2	3.0–6.9
Thianpong et al. [71] (2009)	$12–45 \times 10^3$	Water	Twisted tape in dimpled tubes /6	y = 3, p/d_i = 0.7 δ = 0.5 mm, w = 22 mm, e/d_i = 0.097, d_i = 20.6 mm	5.8–6.3	2.1–3.0
Eiamsa-ard et al. [72] (2010)	$3.7–21 \times 10^3$	Water	Twisted tape/11	y = 2.5, w = 9 mm, δ = 0.8 mm, d_i = 19 mm	5.2–8.4	2.1–2.8
Promvonge et al. [55] (2012)	$6–60 \times 10^3$	Water	Twisted tape in finned tubes /13	y = 8.09, w = 11.5 mm, δ = 1 mm, e/d_i = 0.06, p/d_i = 0.27, d_i = 23 mm	10.4–20.7	3.6–6.2
Eiamsa-ard and Kiatkittipong [73] (2014)	$5–15 \times 10^3$	TiO_2/water	Twisted tapes/7	y = 3.0, CC-QTs 4 tapes, w = 8 mm, δ = 0.8 mm, d_i = 19 mm	10.2–11.4	2.7–3.2

3.3. Experimental data for internally twisted tape and coil

Experimental data on the heat transfer and friction factor of pipes fitted with twisted tape or coil are summarized in Table 4. Reynolds number is less than 100,000. The fluids include water, oil, ethylene glycol, and nanofluids. The experiments with high viscosity oil are mostly in laminar flow. The twist ratio(y) is normally in the range of 2 to ∞. Listed in the table is also for the tube which gives the highest heat transfer enhanced ratio in the paper.

According to Table 4, the increase in friction factor is usually higher than the increase in heat transfer at the same Reynolds number. The maximum increase in heat transfer coefficient is 7.6 times over empty plain tube [69] for the twisted-tape in corrugated tubes, while friction factors are as much as 12 times higher. As can be seen in the table, surface roughness, internal helically integral-fin, corrugated tubes can be combined with twisted tapes to construct compound enhancement techniques. Heat transfer can be further enhanced compared with single effect of the twisted tape.

These experimental data are presented in Figs. 8 and 9. Fig. 8 shows the Nu/Pr^n against Reynolds number for 18 tubes fitted with twisted tapes, and Fig. 9 shows the Fanning friction factor versus Reynolds number. Dittus–Boelter and Fanning equation for plain tube is also presented in Figs. 8 and 9 with the same designation method as for Figs. 4 and 5. In order to confirm the comparison is based on the same reference, experiment data for plain tube reported in each paper is also compared with Dittus–Boelter and Fanning equation. They are found to be in good agreement with the two equations. As shown in Figs. 8 and 9 heat transfer enhanced ratios are generally in the range of 1.5 to 6.0, while the values of friction factor increased significantly compared with heat transfer ratio.

The friction factors for most of pipes fitted with twisted tapes are 2–13 times higher than that of the plain tube. The tubes in [53] fitted with serrated twisted tape gives the maximum increase of friction factor, which is as high as 79 times over empty plain tube. The heat transfer enhancement ratio is 3.7–4.8. Different degrees of higher friction factor are observed for compound enhanced techniques such as twisted tape in finned [2,55], dimpled [71], conical-ring [74], and spirally corrugated [68,69] tubes.

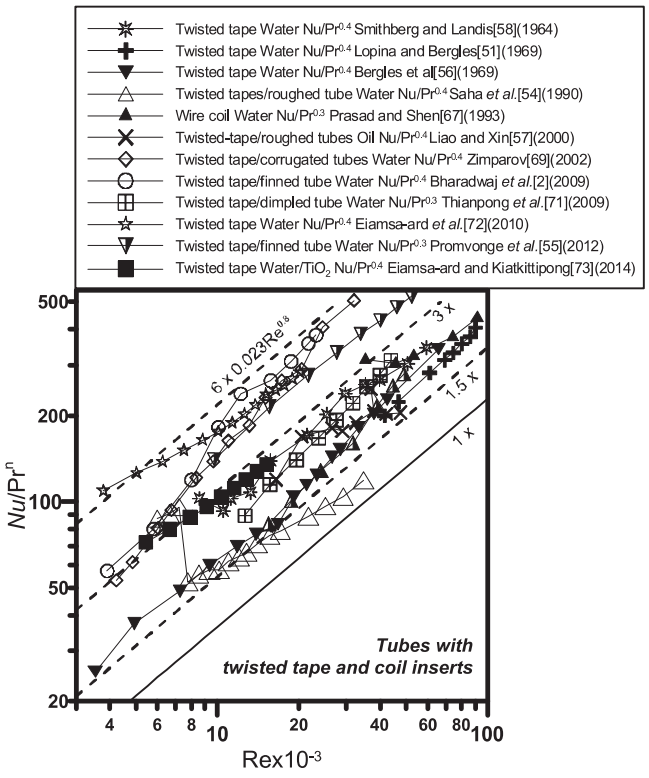

Fig. 8. Experimental data of Nu/Pr^n versus Re for tubes fitted with twisted tape and coil inserts.

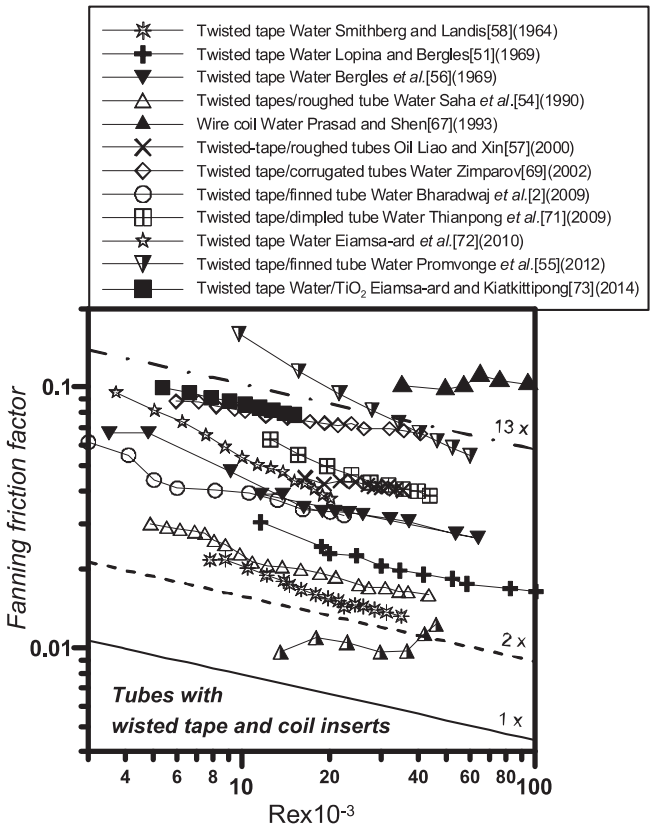

Fig. 9. Experimental data of Fanning friction factor versus Re for tubes with twisted tape and coil inserts.

The curves of Nu/Pr^n versus Reynolds number for different twisted tape tubes have similar slopes as shown in Fig. 8, approaching 0.8 as that of plain tube in the turbulent flow region. The heat transfer enhanced ratio is normally maintained at a certain level for a specific tape inserts in the Reynolds number of $3–100 \times 10^3$. The compound techniques of twisted tape in finned, dimpled, and spirally corrugated tubes have comparably higher heat transfer performance than that of single twisted tapes acting alone. An additional increase up to 300% is observed with the compound technique. At Re = 30,000, the highest Nu/Pr^n reaches up to 500 for the twisted tape inserted in a corrugated tube.

Heat transfer can also be enhanced significantly by counter/co-swirling flow in a tube fitted with twin twisted tapes [72]. At laminar flow, heat transfer coefficients can be increased up to 5-fold according to the measurements of Uttarwar and Raja Rao [66]. However, the heat transfer performance in this region is worse for internally grooved, corrugated, and dimpled tubes according to the previous survey in laminar and transition region [20,75]. According to the investigation of Garcia et al. [75], at Reynolds numbers less than 200, the use of any roughness surface would not produce higher heat transfer coefficients than those produced by plain tube. At Reynolds numbers between 200 and 2000, wire coils had better heat transfer performance than other enhanced techniques and a reliable correlation could be established.

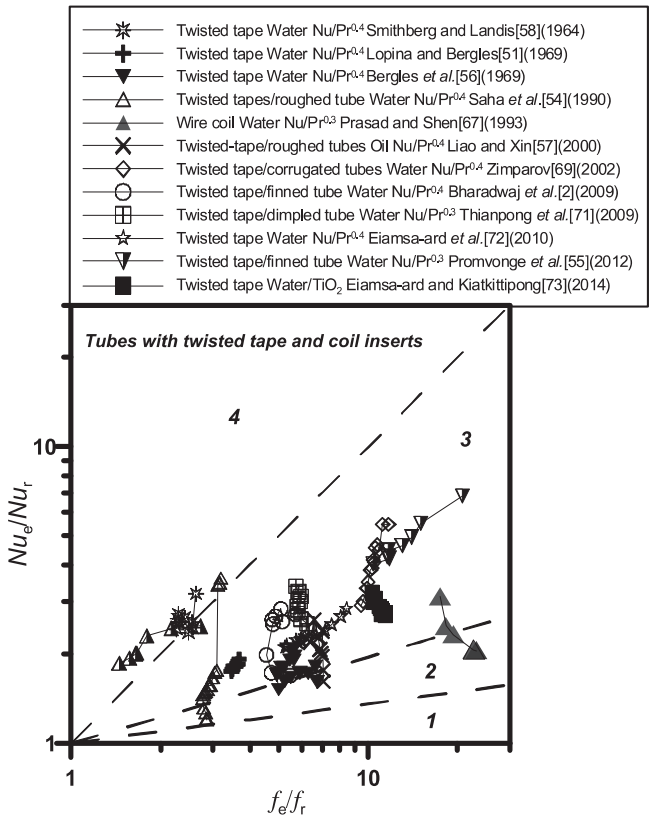

Fig. 10. Performance evaluation plot for tubes with twisted tape and coil inserts.

3.4. Hydraulic-thermal performance evaluation of tape inserts

A comprehensive evaluation on the heat transfer and pressure drop for the tube fitted with internally twisted tapes or coils are presented in the performance evaluation plot (See Fig. 10). For tubes fitted with twisted tapes or coils, most of data falls into Regions 2 and 3, while for internally finned tubes, most of data fall into the region of 3 and 4 in the Reynolds number of 30–100 $\times$ 10^3 (see Fig. 6). This implies that the hydraulic-thermal performance of the internally finned tubes are better than tubes with inserted twisted tapes or coils.

By using the performance evaluation plot, the tube with wire coil inserts in the investigation of Uttarwar and Raja Rao [66] performs better than other tubes in the comparison. The test section geometry used in this experiment is $p/d_i = 0.4$, $e/d_i = 0.079$, $\alpha = 76°$, and $d_i = 25.2$ mm. The tube in the investigation of Prasad and Shen [67] performs worst.

4. Corrugated and twisted tube

4.1. Introduction of corrugated and twisted tube

The "corrugated [76]," "wavy [77]," "spiral indented [78]," "torsion [79]"or "fluted [80]" tubes are produced by deforming

Fig. 11. Corrugated tubes.

plain tube and they may develop secondary circulating flows in a plane normal to the axis of tube. Since the enhancement mechanism of these tubes are more or less the same, in the following discussion we will take the corrugated tube as the example. As shown in Fig. 11, corrugated tubes are shaped into discrete grooves at periodic intervals along the flow direction. The variations of corrugation helical angle may range from 0 to 90°. It can also be further enhanced with multiple-start spiral corrugations and inserts. The enhanced heat transfer and increased friction factor are mainly caused by the higher ridges of corrugated tubes and existence of re-circulating flow regions inside the deep grooves.

The advantage of corrugated tubes is that the fouling is limited and easy to be eliminated compared with the internally finned tubes and inserts. The outside of the corrugated tube also has some enhancement effects for outside fluid convective heat transfer [81]. It's also easier to be produced. The strength and integrity may not be seriously affected by deforming or indenting a plain tube [82]. In the circumstance where the fouling potential and reliability need to be consciously considered, corrugated tube might be a good choice such as in power plant condenser [83]. A comparative study of the three tubes: corrugated, dimpled and wire coils inserted tubes was conducted by Garcia et al. [75]. They found that at Reynolds number range of 2000–10,000, the Nusselt number was similar for the three types of tube, while friction factor of corrugated tube was the lowest. The weakness of corrugated tube might be a lower heat transfer coefficient in laminar flow region [84].

Several parameters are required to predict the thermal–hydraulic performances of the corrugated tubes. The geometry parameters include pitch(p), indent width(w) and maximum height(e) of indent, and starts(N_s) for multi-starts deformation (Fig. 12). The analytical models of friction factor for the corrugated tube are based on the friction similarity law presented by Nikuradse [32] over the artificial roughness. Some heat transfer correlation are based on application of a heat-momentum transfer analogy developed by Dipprey and Sabersky [33]. The application

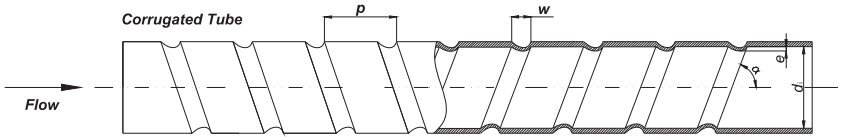

Fig. 12. Illustration of corrugated tube.

of the models on corrugated tubes was analyzed in [82,85]. Nusselt number and friction factor correlations were also derived by best-fitting of experimental data [81,86], while mostly they only give a good agreement with the data from which they were obtained.

4.2. Experimental data on corrugated and twisted tubes

Heat transfer and friction factor test dada for corrugated tubes are summarized in Table 5. For the investigation with more than one tube, only the data for the tube that giving the best heat transfer performance is selected. The basic geometry parameters have following variation range: p/d_i from 0.2 to 2 and e/d_i is from 0.017 to 0.154.

Nu/Pr^n and friction factor are also compared with Dittus–Boelter and Fanning equations in Figs. 13 and 14. The heat transfer enhanced ratios for corrugated tubes are mostly located in the range of 1.5 to 4. The ratios of friction factors are normally in the range of 2 to 6. It can be found from Fig. 13 that fitting of experimental data is almost linear for Nu/Pr^n versus Reynolds number and parallel to the curve of $Re^{0.8}$ in the lg-lg coordinates, meaning that the collected data are mainly in the turbulent flow region. It is similar with the internal integral-fins and twisted tapes inside the tube. For friction factor versus Reynolds number in Fig. 14, as Re increases, friction factor decreases slightly slower than that of the smooth tubes.

For the multi starts tubes in Table 5, pressure drop is substantially increased compared with the heat transfer enhancement. Increases in heat transfer coefficient of up to 380% have been reported for four starts corrugated tube [91]. However, the ratios of friction factor are as much as 4.5 times higher. A remarkable high ratio of friction factor is observed from V-nozzle flow channel. The ratio of friction factors is up to 102 times higher than plain tube, while the heat transfer enhancement is only 2.6–3.0.

The corrugated tubes with lower p/d_i and higher e/d_i usually have higher pressure drop. In the experimental investigations of Zimparov et al. [89], Sethumadhavan and Raja Rao [82], and Cui et al. [80], p/d_i has a lower value around 0.3, the pressure drop increase is higher compared with other tubes. For the tube with

Table 5
Heat transfer and friction factors data of corrugated and twisted tubes.

Researcher	Re	Fluid	Tube/ number	Best tube/feature	f/f_r	Nu/Nu_r
Mimura and Isozaki [87] (1977)	8–40 × 10^3	Water	Corrugated /9	p/d_i = 0.64, e/d_i = 0.078, Ns = 1, d_i = 14.08 mm	2.8–3.5	2.0–2.3
Ganeshan and Raja Rao [88] (1982)	50–90 × 10^3	Water, polymer solutions	Corrugated/7	p/d_i = 1.169, e/d_i = 0.0261, α = 65°, Ns = 1, d_i = 25.66 mm	1.9–2.4	1.8–2.6
Sethumadhavan and Raja Rao [82] (1986)	10–80 × 10^3	Water, EG	Multi starts corrugated /5	p/d_i = 0.297, α = 65°, e/d_i = 0.023, N_s = 4, d_i = 25.26 mm	2.6–3.3	1.6–1.8
Zimparov et al. [89] (1991)	10–70 × 10^3	Water	Corrugated/25	p/d_i = 0.256, α = 84.7°, e/d_i = 0.017, N_s = 1, d_i = 24.97 mm	4.5–5.6	3.0–3.2
Chen et al. [90] (2001)	10–25 × 10^3	Water	Four starts spiral/9	p/d_i = 0.48, α = 61.4°, e/d_i = 0.12, d_i = 18.86 mm	3.7–4.5	2.5–3.8
Yang et al. [91] (2001)	6–93 × 10^3	Water, oil	Corrugated/4	p/d_i = 0.598, α = 79.2° e/d_i = 0.0398, d_i = 20.08 mm	1.4–1.5	1.6–1.7
Cui et al. [80] (2003)	8–30 × 10^3	Water	Corrugated/6	p/d_i = 0.3129, α = 84.32° e/d_i = 0.0409, N_s = 1, d_i = 10.26 mm	3.3–3.9	1.9–2.8
Naphon et al. [92] (2006)	5–25 × 10^3	Water	Corrugated/9	p/d_i = 0.784, α = 45° e/d_i = 0.185, d_i = 8.1 mm	2.4–2.6	2.0–2.2
Pethkool et al. [93] (2011)	5.5–60 × 10^3	Water	Corrugated/9	p/d_i = 0.27, α = 15° e/d_i = 0.06, d_i = 25 mm	1.9–2.1	1.9–3.1
Fernandez-Seara and Uhia [81] (2012)	10–100 × 10^3	Water	Corrugated/9	p/d_i = 0.556, α = 91° e/d_i = 0.044, N_s = 1, d_i = 18 mm	4.3–4.9	2.1–2.4
García et al. [75] (2012)	0.1–100 × 10^3	Water	Corrugated/3	p/d_i = 0.886, e/d_i = 0.057, d_i = 18 mm	1.8–3.8	1.4–2.3
Darzi et al. [86] (2014)	5–20 × 10^3	Water/Al_2O_3	Corrugated/9	p/d_i = 0.617, e/d_i = 0.154, d_i = 8.1 mm	2.5–3.1	2.7–3.2
Kathait and Patil [76] (2014)	7.5–50 × 10^3	Water	Corrugated/4	p/d_i = 0.444, e/d_i = 0.044, d_i = 45 mm	2.5–2.7	1.5–2.6

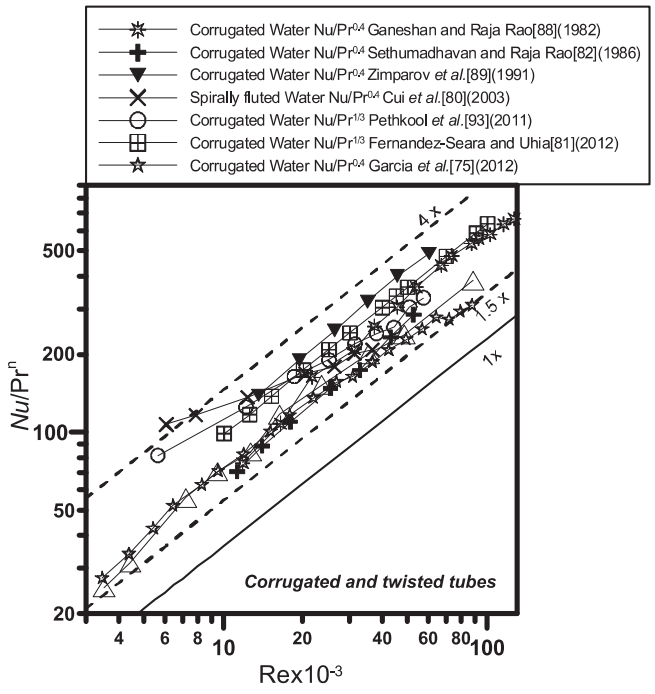

Fig. 13. Experimental data of Nu/Pr^n versus Re of corrugated and twisted tubes.

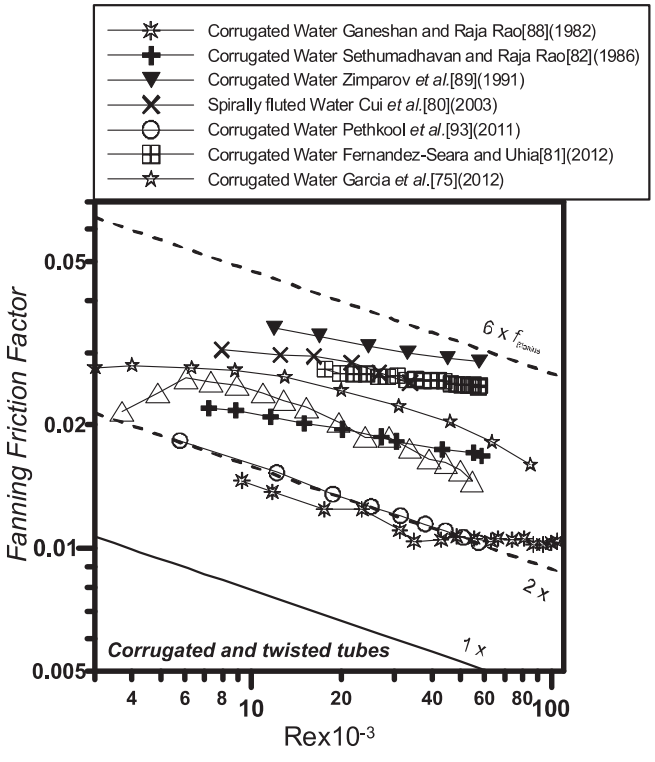

Fig. 14. Experimental data of Fanning friction factor versus Re for corrugated and twisted tubes.

a higher value of $e/d_i = 0.12$ in Chen et al. [90], the pressure drop increase is up to 3.7–4.5. Higher Nusselt number is usually accompanied with large increase of pressure drop, while for one of tubes that gives the best performance in Pethkool et al. [93], heat transfer enhancement is higher than increase of pressure drop, which might be the most favorable case. For most of corrugated tubes,

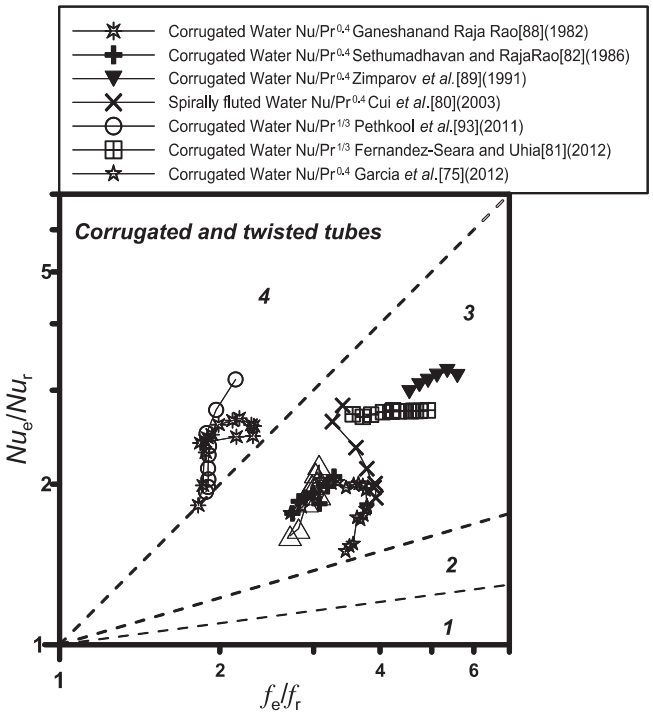

Fig. 15. Performance evaluation plot for corrugated and twisted tubes reported in literature.

the heat transfer enhanced ratio is 1.5 to 4, and friction factor enhanced ratio is 1.8 to 6. Generally, pressure drop for corrugated tubes is at the intermediate position between twisted tape inserts and internal micro-fin tubes. The net enhancement might possibly be achieved with further optimization.

4.3. Hydraulic-thermal performance evaluation of corrugated and twisted tubes

Figure 15 shows the performance evaluation results of the corrugated tubes. Only the data of Ganeshan and Raja Rao [88] and Pethkool et al. [93] are in Region 4, where the heat transfer can be enhanced with identical flow rate. Most of the experimental data locates in Region 3, where heat transfer is enhanced per identical pressure drop. Moreover, most of data in Region 3 are at a position close to the boundary of Region 3 and 4, whereas, for the twisted tape inserts, most of data in Region 3 are very close to the boundary of Region 2 and 3, in the lower part of Region 3, indicating that as whole the hydraulic-thermal performance of the corrugated tube is better than that of twisted tape.

The thermo-hydraulic performance of the corrugated tube in Pethkool et al.[93] is better than other tubes in the comparison. The geometry is characterized by $p/d_i = 0.27$, $\alpha = 15°$, $e/d_i = 0.06$, $d_i = 25$ mm.

5. Dimpled and other three dimensional roughed tube

5.1. Introduction of dimpled and other three dimensional roughed tube

The discontinuous dimples, protrusions and projections in surface are also effective ways to enhance the single-phase convective heat transfer. The protrusions are designed with circular, triangular, rectangular, elliptic or any other cross sections at certain height. In order to reduce additional pressure loss, the shape of protrusions is usually designed with smooth edges. Uniform or random distribution of protrusions with any shape on a heat

transfer surface are often referred as 3-dimensional roughness. The reason for heat transfer enhancement of dimpled tube is the turbulence caused by protrusions. The protrusions contribute the most important part to heat transfer augmentation. It might be used in a variety of industrial applications, such as plate-fin heat exchanger and internal cooling passages of turbine blades.

A typical dimpled tube is shown in Fig. 16. The artificial protrusions inside the tube is produced by dimpling the outside surface. The heat transfer and pressure drop are affected by dimple ratio (e/d_i, the ratio of dimple height to internal diameter), and transverse and axis pitch of dimpled surface. The protrusions might also be arranged along one or more spiral curves. The angle between curve and axis of tube is helix angle (α). The axial distance between two neighbor dimples along one circumferential spiral curve is pitch(p). If the number of curves are more than one, number of curves is called starts (N_s). The heat transfer enhancement and pressure drop increase are affected by the above geometric features and Reynolds number.

The shape of dimpled pipe is not complicated. It's easy to manufacture with lower cost. The fouling of dimpled tubes is also limited and easy to be eliminated compared with internally finned tubes and inserts. It suites for different types of heat exchangers and fluid. The drawback is that the height of protrusions are limited with the restrictions of strength when dimpled from outside of tube. Some vibration and noise problems might be observed.

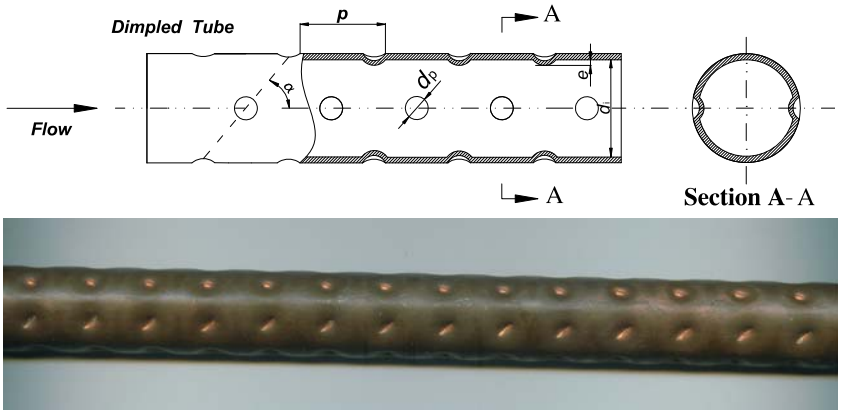

Fig. 16. Schematic diagram and photo of dimpled tube.

Table 6
Heat transfer and friction factor data of dimpled and other three dimensional roughed tubes.

Researcher	Re	Fluid	Tube/ number	Best tube /feature	f/f_r	Nu/Nu_r
Gowen and Smith [94] (1968)	$6–100 \times 10^3$	Air, water, ethylene glycol	Sand roughness /8	$e/d_i = 0.026$, $d_i = 15.88$ mm	3.5–5.8	2.3–3.3
Rabas et al. [95] (1993)	$10–60 \times 10^3$	Water	Dimpled/2	$p/d_i = 1.448$, $e/d_i = 0.0173$, $N_s = 12$, $d_i = 14.71$ mm	1.5–1.9	1.5–1.6
Liao and Xin [96] (1995)	$0.25–7 \times 10^3$	Ethylene glycol	Extended protrusions /7	$p_a/d_i = 0.32$, $p_c/d_i = 0.179$, $e/d_i = 0.04$, $d_i = 13.5$ mm	1.7–4.4	2.6–3.4
Liao et al. [57] (2000)	$5–80 \times 10^3$	Water, ethylene glycol	Extended protrusions /14	$p_a/di = 3.98$, $p_c/d_i = 0.244$, $e/d_i = 0.098$, staggered	3.8–4.4	2.9–3.6
Chen et al. [97] (2001)	$7.5–52 \times 10^3$	Water	Dimpled/6	$p/d_i = 0.602$, $e/d_i = 0.078$ $N_s = 6$, $d_i = 16.6$ mm	3.3–4.8	2.1–2.8
Vicente et al. [98] (2002)	$10–100 \times 10^3$	Water, ethylene glycol	Dimpled/10	$p/d_i = 0.819$, $e/d_i = 0.0988$, $d_i = 16$ mm	3.1–3.5	1.3–2.0
Vicente et al.[99] (2002)	$2–100 \times 10^3$	Water, ethylene glycol	Dimpled/10	$p/d_i = 0.906$, $e/d_i = 0.114$, $d_i = 16$ mm	3.2–4.2	1.5–2.5
Li et al. [100] (2009)	$15–60 \times 10^3$	Water	Discrete ribs/1	$p/d_i = 0.32$, $\alpha = 45°$ $e/d_i = 0.02$, $N_s = 12$, $d_i = 25$ mm	2.8–3.5	2.0–2.1
Webb [101] (2009)	$4–24 \times 10^3$	Water	Coned/3	$p_a/d_i = 3.95$, $p_c/di = 7.21$, $e/d_i = 0.025$, $d_i = 17.32$ mm	3.6–4.6	2.6–4.5
Kukulka et al. [102] (2011)	$2–5 \times 10^3$	Water	Viper tube/6	–	–	1.2–4
Suresh et al. [103] (2011)	$2.5–6 \times 10^3$	Water /CuO	Dimpled/1	$p/d_i = 0.556$, $e/d_i = 0.124$ $d_i = 4.85$ mm	1.0–1.1	1.5–1.7

Because there are numerous configurations of three dimensional protrusions, the predictions of heat transfer and fluid flow are also diversified and complicated. The equations by fitting of experimental data mostly only give a good agreement with the data from which they were derived.

5.2. Experimental data of dimpled and three dimensional roughed tubes

The measurement data of convection heat transfer of circular tubes with the three dimensional protrusions are summarized in Table 6. Totally 78 tubes are reviewed and the best heat transfer tube in each paper is listed in the table. Most of the experiments are conducted in the turbulent flow mainly with water as test fluids. The ratios of p/d_i and e/d_i are in the range of 0.2 to 4 and 0.01 to 0.2, respectively. Tubes in Webb [101] and Liao and Xin [96] give the highest heat transfer enhanced ratios of 4.5. Dimpled tube with twisted tape in Thianpong et al. [71] has the highest increase of friction factor.

The Nusselt number modified by Prandtl number is shown in Fig. 17. The tubes with coned protrusions [101] yield the best heat transfer enhancement ratio at higher Reynolds number. The enhanced ratio for the coned tube is increasing as the increase of Reynolds number. It is followed by the dimpled tubes with twisted tapes and 3-D protrusions by Liao et al. [57]. The dimpled and other tubes with artificial projections have the heat transfer enhanced ratio ranged from 1.5 to 3. The enhanced ratios for most of the dimpled tubes are kept constant in turbulent flow region.

The friction factors of the tubes with internal projections are shown in Fig. 18. A substantial increases of friction factor is observed for dimpled tube with twisted tape inserts. The protrusions with non-circular cross sections and sand blast roughness have higher pressure drop than the other dimpled tubes. The dimpled tubes selected have increased pressure drop ratio of 3–5 over the plain tube.

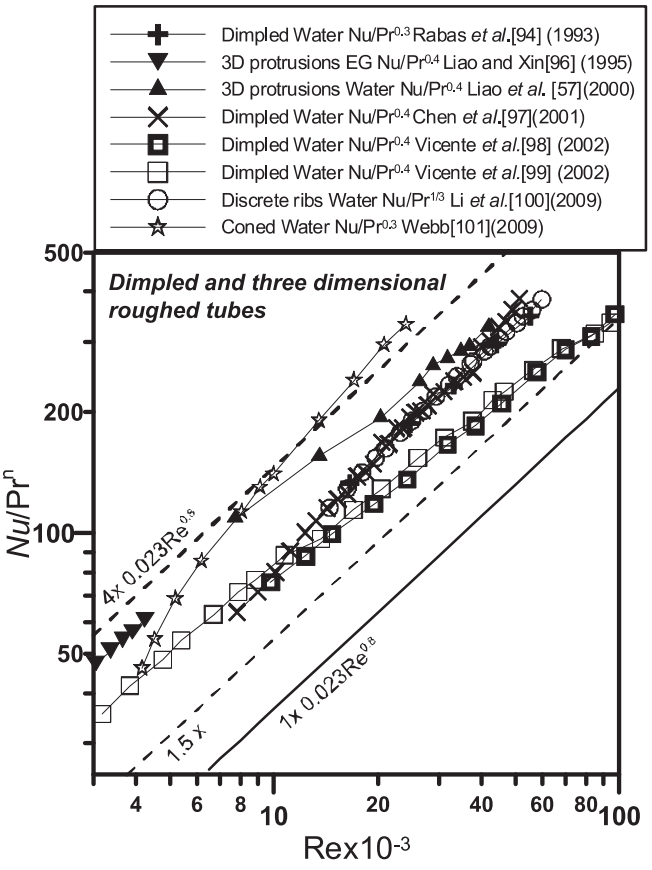

Fig. 17. Experimental data of Nu/Pr^n versus Re of dimpled and three dimensional roughed tube.

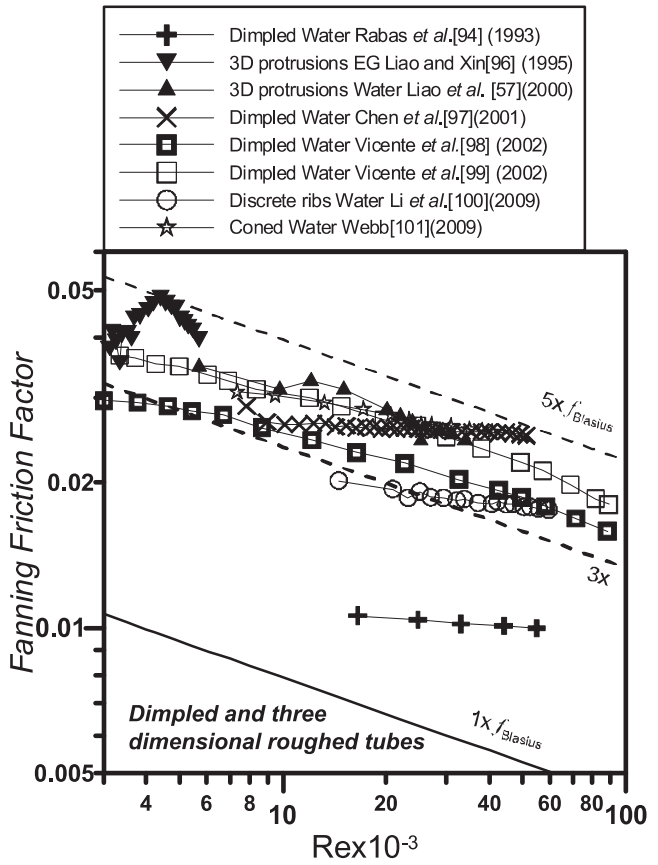

Fig. 18. Experimental data of Fanning friction factor versus Re of dimpled and three dimensional roughed tube.

It might be a widely accepted perception that the sharper-edged profiles tend to increase the turbulence intensity and also contribute to great pressure drop. Thus the pressure drop should reduce for dimpled tube which has gradually changing curvature. However, the friction factor does not reduced too much compared with integral micro-fin and corrugated tubes and may even increase as indicated in Fig. 18. One of the reasons might be that the tubes in Fig. 18 are that give the best performance in each paper, and the author may try to enhance the structure of dimples to obtain higher enhancement, and higher heat transfer enhancement also cause a greater pressure drop. For the tubes with increased protrusions height, the heat transfer and friction may also increase [55]. The diagram in [97] also indicates that the pressure drop penalty will increase with multi-starts.

5.3. Hydraulic-thermal performance evaluation of dimpled and three dimensional roughed tubes

The evaluation plot for dimpled and three-dimensional protrusions are shown in Fig. 19. As show in the figure, the ratios of friction factor mostly are from 3 to 5, and heat transfer enhanced ratios range from 1.5 to 4. The increment of friction factor is generally higher than increment of heat transfer. Only the data of Rabas et al. [95] are in Region 4. The tube of Webb [101] is in the boundary of Region 3 and Region 4. All the other experimental

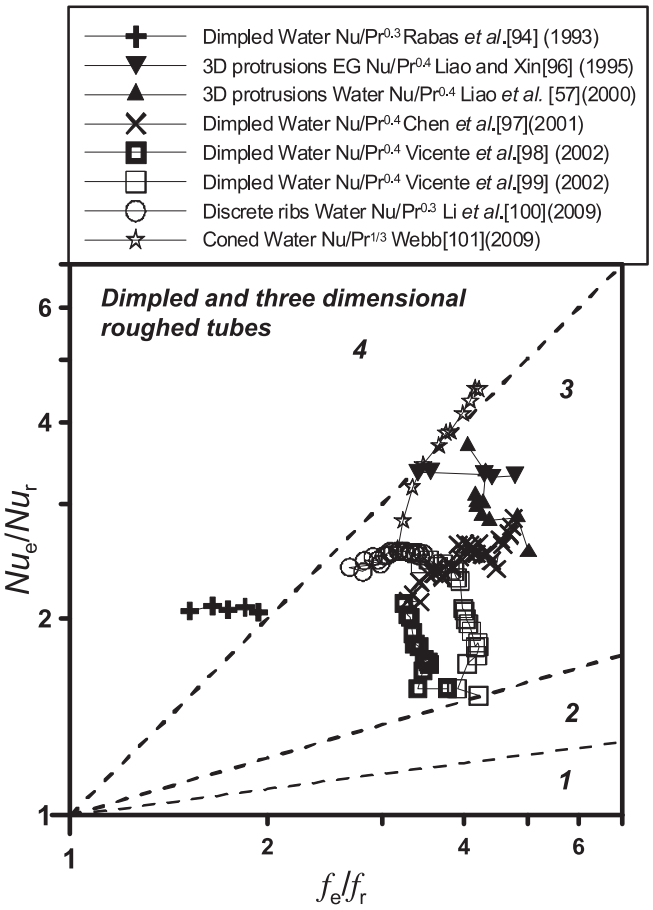

Fig. 19. Performance evaluation plot for dimpled and three dimensional roughed tube reported in literature.

data mainly locate in Region 3. It indicates that dimpled or protruded surface can enhance heat transfer per identical pressure drop.

One notable feature can be observed from Fig. 19 for the three tubes of Vicente et al. [98], Liao et al. [57] and Thianpong et al. [71]: with a bit of increase in friction factor ratio, a remarkably decrease of heat transfer enhancement ratio can be observed. Such variation character should be considered in the design of heat exchanger.

The coned tube in the investigation of Webb [101] has better thermo-hydraulic performance than other tubes in the comparison. The structure parameters of this tube is $p_a/d_i = 3.95$, $p_c/d_i = 7.21$, $e/d_i = 0.025$, $d_i = 17.32$ mm.

It should be noted that the experimental data presented in the evaluation plot are the tube which gives the best heat transfer in each paper. Thus, for each paper some other tube with lower levels of heat transfer enhancement may locate in different region of evaluation plot.

6. Conclusions

A systematic survey and evaluation on the thermal–hydraulic performance of four very common types of enhanced techniques for in-tube heat transfer: internal integral-fin, twisted tape insert, corrugated, dimpled, are conducted in this paper. Compound enhancement techniques, which involves two or more techniques utilized simultaneously are also evaluated. The heat transfer and friction factor of different enhanced techniques of the same type are presented in a same graphs with Re as the abscissa, providing a useful global point of view for heat exchanger design. A useful performance evaluation plot is adopted to identify at what constraint the studied technique can enhance heat transfer. And the best parameters for each type of enhanced structure are identified. The following major conclusions can be drawn:

(1) The enhancement ratio over Dittus–Boelter equation at the same Reynolds number for internal integrally finned tubes are generally in the range of 2–4, inserted twisted tapes are 1.5–6, corrugated tubes is 1.5 to 4 and dimpled tubes is 1.5 to 4, including the compound enhancement techniques. The friction factor increased ratio over Fanning equation are mostly in the range of 1–4 for internal integrally finned tubes, 2–13 for inserted twisted tape, corrugated tubes is 2–6 and dimpled tubes is 3–5.

(2) Internally-finned tubes yield the best thermal–hydraulic performance compared with other three types of enhanced tubes, as a large number of data are located in Region 4 of the performance evaluation plot, indicating that the heat transfer enhancement can be achieved with the same fluid flow rate.

(3) The pressure drop of twisted tape inserts is remarkably increased at the turbulent flow. In the performance evaluation plot most data are located in Region 3 and Region 2. It implies that this kind of enhanced techniques can enhance heat transfer per identical pumping power or identical pressure drop. However, it is found that they are more effective in laminar and transition flow. Thus they may suite to enhance the heat transfer of fluid with high viscosity.

(4) The experimental data of corrugated tubes and dimpled tubes are mostly distributed in Region 3 of the performance evaluation plot, where the enhancement of heat transfer rate can be obtained per identical pressure drop.

(5) Even after numerous investigations in the past half century, completely satisfactory and unified prediction correlations for finned, tape inserted, corrugated, and dimpled surface are still not available in term of geometrical parameters. Considerable disagreement among the studies still exists. Thus further studies are highly needed to obtain practical correlations with deviations acceptable for engineering design.

(6) The tubes of integral-fin in Jensen and Vlakancic [29], twisted tape inserts in Uttarwar and Raja Rao [66], corrugated in Pethkool et al. [93], and dimpled tubes in Webb [101] have better thermo-hydraulic performance than other tubes in the comparison.

Conflict of Interest

None declared.

Acknowledgment

This work was supported by the National Key Basic Research Program of China (973 Program) (2013CB228304, 2011CB707203)

References

[1] S. Al-Fahed, L. Chamra, W. Chakroun, Pressure drop and heat transfer comparison for both microfin tube and twisted-tape inserts in laminar flow, Exp. Thermal Fluid Sci. 18 (4) (1999) 323–333.
[2] P. Bharadwaj, A. Khondge, A. Date, Heat transfer and pressure drop in a spirally grooved tube with twisted tape insert, Int. J. Heat Mass Transfer 52 (7) (2009) 1938–1944.
[3] A.E. Bergles, H.L. Morton, Survey and evaluation of techniques to augment convection heat transfer, Engineering Projects Laboratory Report HTL 5382-34, Massachusetts Institute of Technology, Cambridge, MA.1965.

[4] A.E. Bergles, R.L. Webb, G.H. Junkhan, Energy conservation via heat transfer enhancement, Energy 4 (1979) 193–200.
[5] R.L. Webb, A.E. Bergles, Heat transfer enhancement: second generation technology, Mech. Eng. 105 (6) (1983) 60–67.
[6] R.L. Webb, Enhancement of single phase heat transfer, in: S. Kakac, R.K. Shah, W. Aung (Eds.), Handbook of Single Phase Heat Transfer, Wiley, New York, 1987. Chapter 17.
[7] R.L. Webb, K. Menze, T. Ruddy, Z. Ayub, M. Fujii, Techology review, J. Enhanced Heat Transfer 1 (2) (1994) 127–130.
[8] A.E. Bergles, M.K. Jenson, B. Shome, The literature on enhancement of convective heat and mass transfer, J. Enhanced Heat Transfer 4 (1) (1996) 1–6.
[9] A.E. Bergles, Heat transfer enhancement - The maturing of second-generation heat transfer technology, Heat Transfer Eng. 18 (1) (1997) 47–55.
[10] A.E. Bergles, Enhanced heat transfer: Endless frontier, or mature and routine?, J Enhanced Heat Transfer 6 (2–4) (1999) 79–88.
[11] A.E. Bergles, ExHFT for fourth generation heat transfer technology, Exp. Thermal Fluid Sci. 26 (2–4) (2002) 335–344.
[12] R.M. Manglik, A.E. Bergles, Enhanced heat and mass transfer in the new millennium: A review of the 2001 literature, J. Enhanced Heat Transfer 11 (2) (2004) 87–118.
[13] Z.X. Li, Z.Y. Guo, Optimization principles for heat convection, in: L.Q. Wang (Ed.), Advances in Transport Phenomena 2010, Springer-Verlag, Berlin Herderberg, 2011.
[14] A.E. Bergles, Recent developments in enhanced heat transfer, Heat Mass Transfer 47 (2011) 1001–1008.
[15] R.M. Manglik, Heat transfer enhancement, in: A. Bejan, A. Kraus (Eds.), Heat Transfer Handbook, John Wiley Sons Inc, Hoboken, 2003, pp. 1029–1130. Chapter 14.
[16] A.E. Bergles, Techniques to enhance heat transfer, in: W.M. Rohsenow, J.P. Hartnett, Y.I. Cho (Eds.), Handbook of Heat Transfer, third ed., McGraw-Hill, New York, 1998. Chapter 11.
[17] J.F. Fan, W.K. Ding, J.F. Zhang, Y.L. He, W.Q. Tao, A performance evaluation plot of enhanced heat transfer techniques oriented for energy-saving, Int. J. Heat Mass Transfer 52 (1) (2009) 33–44.
[18] Q. Li, G. Flamant, X. Yuan, P. Neveu, L. Luo, Compact heat exchanger: a review and future applications of new generation of high temperature solar receivers, Renewable Sustainable Energy Rev. 15 (2011) 4855–4875.
[19] Ya-Ling He, Wen-Quan Tao, Convective heat transfer enhancement: mechanism, techniques and performance evaluation, in: E.M. Sparrow, Y.I. Cho, J.P. Abraham, J.M. Gorman (Eds.), Adv. in Heat Transfer, 46, 2014, pp. 87–186.
[20] X.W. Li, J.A. Meng, Z.X. Li, Experimental study of single-phase pressure drop and heat transfer in a micro-fin tube, Exp. Thermal Fluid Sci. 32 (2) (2007) 641–648.
[21] J. Vogel, J. Eaton, Combined heat transfer and fluid dynamic measurements downstream of a backward-facing step, J. Heat Transfer 107 (4) (1985) 922–929.
[22] J.-H. Kim, K.E. Jansen, M.K. Jensen, Analysis of heat transfer characteristics in internally finned tubes, Numer. Heat Transfer, Part A: Appl. 46 (1) (2004) 1–21.
[23] D. Ryu, D. Choi, V. Patel, Analysis of turbulent flow in channels roughened by two-dimensional ribs and three-dimensional blocks. Part I: resistance, Int. J. Heat Fluid Flow 28 (5) (2007) 1098–1111.
[24] D. Ryu, D. Choi, V. Patel, Analysis of turbulent flow in channels roughened by two-dimensional ribs and three-dimensional blocks. Part II: heat transfer, Int. J. Heat Fluid Flow 28 (5) (2007) 1112–1124.
[25] C.-H. Liu, T.N. Chung, Forced convective heat transfer over ribs at various separation, Int. J. Heat Mass Transfer 55 (19) (2012) 5111–5119.
[26] R.L. Webb, E.R.G. Eckert, R.J. Goldstein, Heat transfer and friction in tubes with repeated-rib roughness, Int. J. Heat Mass Transfer 14 (4) (1971) 601–617.
[27] T.S. Ravigururajan, A.E. Bergles, Development and verification of general correlations for pressure drop and heat transfer in single-phase turbulent flow in enhanced tubes, Exp. Thermal Fluid Sci. 13 (1) (1996) 55–70.
[28] R.L. Webb, N.H. Kim, Principle of Enhanced Heat Transfer, second ed., Taylor & Francis, Boca Raton, 2005.
[29] M.K. Jensen, A. Vlakancic, Experimental investigation of turbulent heat transfer and fluid flow in internally finned tubes, Int. J. Heat Mass Transfer 42 (7) (1999) 1343–1351.
[30] G.J. Zdaniuk, L.M. Chamra, P.J. Mago, Experimental determination of heat transfer and friction in helically-finned tubes, Exp. Thermal Fluid Sci. 32 (3) (2008) 761–775.
[31] G. Tanda, Effect of rib spacing on heat transfer and friction in a rectangular channel with 45 angled rib turbulators on one/two walls, Int. J. Heat Mass Transfer 54 (5) (2011) 1081–1090.
[32] J. Nikuradse, Laws of Flow in Rough Pipes, National Advisory Commission for Aeronautics, Washington, DC, USA, 1950.
[33] D.F. Dipprey, R.H. Sabersky, Heat and momentum transfer in smooth and rough tubes at various Prandtl numbers, Int. J. Heat Mass Transfer 6 (5) (1963) 329–353.
[34] J. Han, L. Glicksman, W. Rohsenow, An investigation of heat transfer and friction for rib-roughened surfaces, Int. J. Heat Mass Transfer 21 (8) (1978) 1143–1156.
[35] D.L. Gee, R. Webb, Forced convection heat transfer in helically rib-roughened tubes, Int. J. Heat Mass Transfer 23 (8) (1980) 1127–1136.
[36] C.C. Wang, C. Chiou, D.C. Lu, Single-phase heat transfer and flow friction correlations for microfin tubes, Int. J. Heat Fluid Flow 17 (5) (1996) 500–508.
[37] T. Carnavos, Heat transfer performance of internally finned tubes in turbulent flow, Heat Transfer Eng. 1 (4) (1980) 32–37.
[38] R.L. Webb, R. Narayanamurthy, P. Thors, Heat transfer and friction characteristics of internal helical-rib roughness, ASME J. Heat Transfer 122 (1) (2000) 134–142.
[39] H. Wang, J. Rose, Prediction of effective friction factors for single-phase flow in horizontal microfin tubes, Int. J. Refrig. 27 (8) (2004) 904–913.
[40] W.T. Ji, D.C. Zhang, Y.L. He, W.Q. Tao, Prediction of fully developed turbulent heat transfer of internal helically ribbed tubes-An extension of Gnielinski equation, Int. J. Heat Mass Transfer 55 (4) (2011) 1375–1384.
[41] B. Kader, A. Yaglom, Turbulent heat and mass transfer from a wall with parallel roughness ridges, Int. J. Heat Mass Transfer 20 (4) (1977) 345–357.
[42] L.J. Brognaux, R.L. Webb, L.M. Chamra, B.Y. Chung, Single-phase heat transfer in micro-fin tubes, Int. J. Heat Mass Transfer 40 (18) (1997) 4345–4357.
[43] J.B. Copetti, M.H. Macagnan, D. de Souza, R.D.C. Oliveski, Experiments with micro-fin tube in single phase, Int. J. Refrig. 27 (8) (2004) 876–883.
[44] D.H. Han, K.-J. Lee, Single-phase heat transfer and flow characteristics of micro-fin tubes, Appl. Thermal Eng. 25 (11) (2005) 1657–1669.
[45] P. Naphon, P. Sriromruln, Single-phase heat transfer and pressure drop in the micro-fin tubes with coiled wire insert, Int. Commun. Heat Mass Transfer 33 (2) (2006) 176–183.
[46] M. Siddique, M. Alhazmy, Experimental study of turbulent single-phase flow and heat transfer inside a micro-finned tube, Int. J. Refrig. 31 (2) (2008) 234–241.
[47] P. Nagarajan, Y. Mukkamala, P. Sivashanmugam, Studies on heat transfer and friction factor characteristics of turbulent flow through a micro-finned tube fitted with left–right inserts, Appl. Thermal Eng. 30 (13) (2010) 1666–1672.
[48] S. Eiamsa-ard, K. Wongcharee, Single-phase heat transfer of CuO/water nanofluids in micro-fin tube equipped with dual twisted-tapes, Int. Commun. Heat Mass Transfer 39 (9) (2012) 1453–1459.
[49] S. Eiamsa-Ard, K. Wongcharee, Heat transfer characteristics in micro-fin tube equipped with double twisted tapes: Effect of twisted tape and micro-fin tube arrangements, J. Hydrodyn. Ser. B 25 (2) (2013) 205–214.
[50] E.P. Bandarra Filho, J.M. Saiz Jabardo, Experimental study of the thermal hydraulic performance of sub-cooled refrigerants flowing in smooth, micro-fin and herringbone tubes, Appl. Thermal Eng. 62 (2) (2014) 461–469.
[51] R. Lopina, A. Bergles, Heat transfer and pressure drop in tape-generated swirl flow of single-phase water, J. Heat Transfer 91 (3) (1969) 434–441.
[52] W.M. Chakroun, S.F. Al-Fahed, The effect of twisted-tape width on heat transfer and pressure drop for fully developed laminar flow, J. Eng. Gas Turbines Power 118 (3) (1996) 584–589.
[53] S.W. Chang, Y.J. Jan, J.S. Liou, Turbulent heat transfer and pressure drop in tube fitted with serrated twisted tape, Int. J. Thermal Sci. 46 (5) (2007) 506–518.
[54] S. Saha, U. Gaitonde, A. Date, Heat transfer and pressure drop characteristics of turbulent flow in a circular tube fitted with regularly spaced twisted-tape elements, Exp. Thermal Fluid Sci. 3 (6) (1990) 632–640.
[55] P. Promvonge, S. Pethkool, M. Pimsarn, C. Thianpong, Heat transfer augmentation in a helical-ribbed tube with double twisted tape inserts, Int. Commun. Heat Mass Transfer 39 (7) (2012) 953–959.
[56] A. Bergles, R. Lee, B. Mikic, Heat transfer in rough tubes with tape-generated swirl flow, ASME J. Heat Transfer 91 (3) (1969) 443–445.
[57] Q. Liao, M. Xin, Augmentation of convective heat transfer inside tubes with three-dimensional internal extended surfaces and twisted-tape inserts, Chem. Eng. J. 78 (2) (2000) 95–105.
[58] E. Smithberg, F. Landis, Friction and forced convection heat-transfer characteristics in tubes with twisted tape swirl generators, ASME J. Heat Transfer 86 (1) (1964) 39–48.
[59] R.M. Manglik, A.E. Bergles, Heat transfer and pressure drop correlations for twisted-tape inserts in isothermal tubes: Part II—Transition and turbulent flows, ASME J. Heat Transfer 115 (4) (1993) 890–896.
[60] R.M. Manglik, A.E. Bergles, Heat transfer and pressure drop correlations for twisted-tape inserts in isothermal tubes: part I—laminar flows, ASME J. Heat Transfer 115 (4) (1993) 881–889.
[61] S. Hong, A. Bergles, Augmentation of laminar flow heat transfer in tubes by means of twisted-tape inserts, ASME J. Heat Transfer 98 (2) (1976) 251–256.
[62] S. Churchill, R. Usagi, A general expression for the correlation of rates of transfer and other phenomena, AIChE J. 18 (6) (1972) 1121–1128.
[63] A. Date, Prediction of fully-developed flow in a tube containing a twisted-tape, Int. J. Heat Mass Transfer 17 (8) (1974) 845–859.
[64] P. Naphon, Heat transfer and pressure drop in the horizontal double pipes with and without twisted tape insert, Int. Commun. Heat Mass Transfer 33 (2) (2006) 166–175.
[65] H. Bas, V. Ozceyhan, Heat transfer enhancement in a tube with twisted tape inserts placed separately from the tube wall, Exp. Thermal Fluid Sci. 41 (2012) 51–58.
[66] S. Uttarwar, M.R. Rao, Augmentation of laminar flow heat transfer in tubes by means of wire coil inserts, ASME J. Heat Transfer 107 (4) (1985) 930–935.
[67] R. Prasad, J. Shen, Performance evaluation of convective heat transfer enhancement devices using exergy analysis, Int. J. Heat Mass Transfer 36 (17) (1993) 4193–4197.
[68] V. Zimparov, Enhancement of heat transfer by a combination of three-start spirally corrugated tubes with a twisted tape, Int. J. Heat Mass Transfer 44 (3) (2001) 551–574.

[69] V. Zimparov, Enhancement of heat transfer by a combination of a single-start spirally corrugated tubes with a twisted tape, Exp. Thermal Fluid Sci. 25 (7) (2002) 535–546.
[70] P. Sivashanmugam, S. Suresh, Experimental studies on heat transfer and friction factor characteristics of laminar flow through a circular tube fitted with regularly spaced helical screw-tape inserts, Exp. Thermal Fluid Sci. 31 (4) (2007) 301–308.
[71] C. Thianpong, P. Eiamsa-Ard, K. Wongcharee, S. Eiamsa-Ard, Compound heat transfer enhancement of a dimpled tube with a twisted tape swirl generator, Int. Commun. Heat Mass Transfer 36 (7) (2009) 698–704.
[72] S. Eiamsa-Ard, C. Thianpong, P. Eiamsa-Ard, Turbulent heat transfer enhancement by counter/co-swirling flow in a tube fitted with twin twisted tapes, Exp. Thermal Fluid Sci. 34 (1) (2010) 53–62.
[73] S. Eiamsa-ard, K. Kiatkittipong, Heat transfer enhancement by multiple twisted tape inserts and TiO2/water nanofluid, Appl. Thermal Eng. 70 (1) (2014) 896–924.
[74] P. Promvonge, S. Eiamsa-ard, Heat transfer behaviors in a tube with combined conical-ring and twisted-tape insert, Int. Commun. Heat Mass Transfer 34 (7) (2007) 849–859.
[75] A. Garcia, J. Solano, P. Vicente, A. Viedma, The influence of artificial roughness shape on heat transfer enhancement: corrugated tubes, dimpled tubes and wire coils, Appl. Thermal Eng. 35 (2012) 196–201.
[76] P.S. Kathait, A.K. Patil, Thermo-hydraulic performance of a heat exchanger tube with discrete corrugations, Appl. Thermal Eng. 66 (1) (2014) 162–170.
[77] K. Bilen, M. Cetin, H. Gul, T. Balta, The investigation of groove geometry effect on heat transfer for internally grooved tubes, Appl. Thermal Eng. 29 (4) (2009) 753–761.
[78] J. Yang, L. Ma, J. Liu, W. Liu, Thermal–hydraulic performance of a novel shell-and-tube oil cooler with multi-fields synergy analysis, Int. J. Heat Mass Transfer 77 (2014) 928–939.
[79] M. Germano, On the effect of torsion on a helical pipe flow, J. Fluid Mech. 125 (1982) 1–8.
[80] H. Cui, X. Yuan, Z. Yao, Experimental investigation of heat transfer and pressure drop characteristics of w-type spirally fluted tubes, Experimental Heat Transfer 16 (3) (2003) 159–169.
[81] J. Fernández-Seara, F.J. Uhía, Heat transfer and friction characteristics of spirally corrugated tubes for outer ammonia condensation, Int. J. Refrig. 35 (7) (2012) 2022–2032.
[82] R. Sethumadhavan, M.R. Rao, Turbulent flow friction and heat transfer characteristics of single-and multistart spirally enhanced tubes, ASME J. Heat Transfer 108 (1) (1986) 55–61.
[83] T.J. Rabas, J. Taborek, Heat-rate improvements obtained by retubing condensers with new, enhanced tube types, J. Enhanced Heat Transfer 3 (2) (1996) 83–94.
[84] P. Vicente, A. Garcıa, A. Viedma, Mixed convection heat transfer and isothermal pressure drop in corrugated tubes for laminar and transition flow, Int. Commun. Heat Mass Transfer 31 (5) (2004) 651–662.
[85] M. Vulchanov, V. Zimparov, L. Delov, Heat transfer and friction characteristics of spirally corrugated tubes for power plant condensers–2. a mixing-length model for predicting fluid friction and heat transfer, Int. J. Heat Mass Transfer 34 (9) (1991) 2199–2206.
[86] A.A. Rabienataj Darzi, M. Farhadi, K. Sedighi, Experimental investigation of convective heat transfer and friction factor of Al2o3/water nanofluid in helically corrugated tube, Exp. Thermal Fluid Science 57 (2014) 188–199.
[87] K. Mimura, A. Isozaki, Heat transfer and pressure drop of corrugated tubes, Desalination 22 (1) (1977) 131–139.
[88] S. Ganeshan, M.R. Rao, Studies on thermohydraulics of single-and multi-start spirally corrugated tubes for water and time-independent power law fluids, Int. J. Heat Mass Transfer 25 (7) (1982) 1013–1022.
[89] V.D. Zimparov, N.L. Vulchanov, L.B. Delov, Heat transfer and friction characteristics of spirally corrugated tubes for power plant condensers–1. experimental investigation and performance evaluation, Int. J. Heat Mass Transfer 34 (9) (1991) 2187–2197.
[90] X. Chen, X. Xu, S. Nguang, A.E. Bergles, Characterization of the effect of corrugation angles on hydrodynamic and heat transfer performance of four-start spiral tubes, ASME J. Heat Transfer 123 (6) (2001) 1149–1158.
[91] D. Yang, H.X. Li, T. Chen, Pressure drop, heat transfer and performance of single-phase turbulent flow in spirally corrugated tubes, Exp. Thermal Fluid Sci. 24 (3) (2001) 131–138.
[92] P. Naphon, M. Nuchjapo, J. Kurujareon, Tube side heat transfer coefficient and friction factor characteristics of horizontal tubes with helical rib, Energy Convers. Manage. 47 (18–19) (2006) 3031–3044.
[93] S. Pethkool, S. Eiamsa-Ard, S. Kwankaomeng, P. Promvonge, Turbulent heat transfer enhancement in a heat exchanger using helically corrugated tube, Int. Commun. Heat Mass Transfer 38 (3) (2011) 340–347.
[94] R. Gowen, J. Smith, Turbulent heat transfer from smooth and rough surfaces, Int. J. Heat Mass Transfer 11 (11) (1968) 1657–1674.
[95] T.J. Rabas, R.L. Webb, P. Thors, N.-K. Kim, Influence of roughness shape and spacing on the performance of three-dimensional helically dimpled tubes, J. Enhanced Heat Transfer 1 (1) (1993).
[96] Q. Liao, M. Xin, Experimental investigation on forced convective heat transfer and pressure drop of ethylene glycol in tubes with three-dimensional internally extended surface, Exp. Thermal Fluid Sci. 11 (4) (1995) 343–347.
[97] J. Chen, H. Müller-Steinhagen, G.G. Duffy, Heat transfer enhancement in dimpled tubes, Appl. Thermal Eng. 21 (5) (2001) 535–547.
[98] P.G. Vicente, A. Garćıa, A. Viedma, Experimental study of mixed convection and pressure drop in helically dimpled tubes for laminar and transition flow, Int. J. Heat Mass Transfer 45 (26) (2002) 5091–5105.
[99] P.G. Vicente, A. Garćıa, A. Viedma, Heat transfer and pressure drop for low Reynolds turbulent flow in helically dimpled tubes, Int. J. Heat Mass Transfer 45 (3) (2002) 543–553.
[100] X.-W. Li, J.-A. Meng, Z.-Y. Guo, Turbulent flow and heat transfer in discrete double inclined ribs tube, Int. J. Heat Mass Transfer 52 (3) (2009) 962–970.
[101] R.L. Webb, Single-phase heat transfer, friction, and fouling characteristics of three-dimensional cone roughness in tube flow, Int. J. Heat Mass Transfer 52 (11–12) (2009) 2624–2631.
[102] D.J. Kukulka, R. Smith, K.G. Fuller, Development and evaluation of enhanced heat transfer tubes, Appl. Thermal Eng. 31 (13) (2011) 2141–2145.
[103] S. Suresh, M. Chandrasekar, S. Chandra Sekhar, Experimental studies on heat transfer and friction factor characteristics of CuO/water nanofluid under turbulent flow in a helically dimpled tube, Exp. Thermal Fluid Sci. 35 (3) (2011) 542–549.